

Caspase-8 Acts as a Molecular Rheostat To Limit RIPK1- and MyD88-Mediated Dendritic Cell Activation

This information is current as of May 13, 2014.

Carla M. Cuda, Alexander V. Misharin, Angelica K. Gierut, Rana Saber, G. Kenneth Haines III, Jack Hutcheson, Stephen M. Hedrick, Chandra Mohan, G. Scott Budinger, Christian Stehlik and Harris Perlman

J Immunol published online 7 May 2014

<http://www.jimmunol.org/content/early/2014/05/07/jimmunol.1400122>

Supplementary Material <http://www.jimmunol.org/content/suppl/2014/05/07/jimmunol.1400122.DCSupplemental.html>

Subscriptions Information about subscribing to *The Journal of Immunology* is online at: <http://jimmunol.org/subscriptions>

Permissions Submit copyright permission requests at: <http://www.aai.org/ji/copyright.html>

Email Alerts Receive free email-alerts when new articles cite this article. Sign up at: <http://jimmunol.org/cgi/alerts/etoc>

Caspase-8 Acts as a Molecular Rheostat To Limit RIPK1- and MyD88-Mediated Dendritic Cell Activation

Carla M. Cuda,* Alexander V. Misharin,* Angelica K. Gierut,* Rana Saber,*
G. Kenneth Haines, III,[†] Jack Hutcheson,[‡] Stephen M. Hedrick,[§] Chandra Mohan,[‡]
G. Scott Budinger,[¶] Christian Stehlik,* and Harris Perlman*

Caspase-8, an executioner enzyme in the death receptor pathway, was shown to initiate apoptosis and suppress necroptosis. In this study, we identify a novel, cell death-independent role for caspase-8 in dendritic cells (DCs): DC-specific expression of caspase-8 prevents the onset of systemic autoimmunity. Failure to express caspase-8 has no effect on the lifespan of DCs but instead leads to an enhanced intrinsic activation and, subsequently, more mature and autoreactive lymphocytes. Uncontrolled TLR activation in a RIPK1-dependent manner is responsible for the enhanced functionality of caspase-8-deficient DCs, because deletion of the TLR-signaling mediator, MyD88, ameliorates systemic autoimmunity induced by caspase-8 deficiency. Taken together, these data demonstrate that caspase-8 functions in a cell type-specific manner and acts uniquely in DCs to maintain tolerance. *The Journal of Immunology*, 2014, 192: 000–000.

Activation of cell surface death receptors (DRs) can initiate two essential death pathways responsible for cell turnover, apoptosis or necroptosis, depending on the cytosolic milieu. Aggregation of a DR (Fas, TNFR1) with its ligand facilitates recruitment of Fas-associated death domain (FADD). FADD then recruits the cysteine–aspartic acid enzyme procaspase-8, which becomes catalytically active by forming a homodimer that initiates the degradative phase of apoptosis through subsequent activation of caspase 3/7 (1). In the absence of FADD or caspase-8, apoptosis is prevented; however, under these conditions, receptor-interacting serine–threonine kinase (RIPK)1–RIPK3 signaling proceeds unchecked, leading to necroptosis (2). However, when cFLIP is present at sufficient levels, this catalytically inactive homolog of caspase-8 forms a heterodimer with caspase-8 that not only prevents apoptosis but also limits RIPK1–RIPK3 necrosome activity (2).

Although caspase-8 is known to function in cell death, conditional deletion studies implicate caspase-8 in a number of cell death-independent activities, including cell motility (3), metastasis (4), suppression of inflammation (5, 6), and NF- κ B activation (7). The current paradigm for these alternate roles for caspase-8 is that they are the consequences of unleashed necroptosis (8, 9). However, a number of recent studies point to the idea that caspase-8 may function in an entirely cell death-independent manner. TLR engagement can provoke RIPK signaling independent of DR activation, thereby leading to formation of a ripoptosome, a complex containing similar proteins involved in necroptosis, including caspase-8, RIPK1, cFLIP, and FADD (10). Additionally, ripoptosome and RIPK3 activity were shown to induce production of proinflammatory cytokine IL-1 β in a caspase-8-dependent manner (11) independent of cell death. Activation of most TLRs requires the adaptor MyD88, which may lead to the phosphorylation and nuclear translocation of transcription factors IFN regulatory factors (IRFs), causing upregulation of proinflammatory gene expression (12). Previous studies showed that caspase-8 cleaves IRF3, targeting it for degradation and dampening TLR-dependent downstream gene induction (13). Taken together, these data suggest that heightened IRF3 transcriptional activity in the absence of caspase-8 may lead to hyperexpression of deleterious downstream IRF3-specific genes.

The vast majority of studies on the Fas-signaling pathway in the immune system and its role in apoptosis and necroptosis have focused on lymphocytes. Loss of Fas in lymphocytes has led to conflicting results (14–16), whereas deletion of caspase-8 yields lymphopenic mice as the result of a failure in proliferation and increased necroptosis (17). Although the phenotype of global and T cell-specific caspase-8 deletion is reversed by RIPK3 deficiency, which suggests that necroptosis is the underlying cause (18), a systemic autoimmunity develops that is similar to germline knockout of Fas (2, 17, 19). Because conditional deletion of Fas or caspase-8 in lymphocytes results in opposite phenotypes, and loss of Fas in dendritic cells (DCs) or overexpression of the general caspase inhibitor p35 in DCs induces a systemic autoimmune disease (14, 20), we investigated the role that caspase-8 plays in DC development and in maintaining tolerance.

*Division of Rheumatology, Department of Medicine, Feinberg School of Medicine, Northwestern University, Chicago, IL 60611; [†]Department of Pathology, School of Medicine, Yale University, New Haven, CT 06510; [‡]Division of Rheumatology, Department of Medicine, University of Texas Southwestern Medical Center, Dallas, TX 75390; [§]Division of Biological Sciences, Department of Cellular and Molecular Medicine, University of California, San Diego, La Jolla, CA 92093; and [¶]Division of Pulmonary and Critical Care, Department of Medicine, Feinberg School of Medicine, Northwestern University, Chicago, IL 60611

Received for publication January 17, 2014. Accepted for publication April 7, 2014.

This work was supported by National Institutes of Health Grant AR060169 (to C.M.C.), Grants AR055600, AI039824, and AR050812 (to C.M.), Grants AI092490 and GM071723 (to C.S.), and Grants AR050250, AR054796, AR055503, and AI067590 (to H.P.), as well as by funds provided by the Solovy-Arthritis Research Society Chair in Medicine (to H.P.).

Address correspondence and reprint requests to Dr. Harris Perlman, Division of Rheumatology, Department of Medicine, Feinberg School of Medicine, Northwestern University, 240 East Huron Street, Room M338, Chicago, IL 60611. E-mail address: h-perlman@northwestern.edu

The online version of this article contains supplemental material.

Abbreviations used in this article: B6, C57BL/6; BMDC, bone marrow-derived dendritic cell; DC, dendritic cell; DR, death receptor; FADD, Fas-associated death domain; IRF, IFN regulatory factor; 1-MT, 1-methyl-D-tryptophan; PAS, periodic acid–Schiff; RIPK, receptor-interacting serine–threonine kinase; SLE, systemic lupus erythematosus; WT, wild-type.

Copyright © 2014 by The American Association of Immunologists, Inc. 0022-1767/14/\$16.00

Specific deletion of caspase-8 in DCs ($Cre^{CD11c}Casp8^{fl/fl}$) is sufficient to induce a systemic autoimmune disease reminiscent of systemic lupus erythematosus (SLE) that is not a consequence of unleashed necroptosis, because this break in tolerance is neither ameliorated nor exacerbated by RIPK3 deletion. $Cre^{CD11c}Casp8^{fl/fl}$ DCs do not display a survival advantage, indicating that defective DC apoptosis is not the underlying cause of the observed inflammation. However, these DCs possess a heightened costimulatory capacity and an elevated response to TLR signaling that is abrogated by RIPK1 inhibition. Interestingly, IRF3 deletion in $Cre^{CD11c}Casp8^{fl/fl}$ mice exacerbates the observed break in tolerance. In contrast, concurrent deletion of caspase-8 and MyD88 in DCs abates both the lymphoproliferative and end-organ disease in $MyD88^{fl/fl}Cre^{CD11c}Casp8^{fl/fl}$ mice. Thus, these data demonstrate that caspase-8 in DCs maintains tolerance in a manner that is independent of cell death and IRF3 but requires dampening of RIPK1 and MyD88 signaling.

Materials and Methods

Mice

C57BL/6 (B6) mice homozygous for loxP-flanked caspase-8 allele ($Casp8^{fl/fl}$) (21) were crossed with mice expressing Cre under control of the CD11c promoter (Cre^{CD11c} ; The Jackson Laboratory, stock number 007567), generating $Cre^{CD11c}Casp8^{fl/fl}$ mice. PCR on FACS-sorted splenic conventional DC populations ($B220^{-}CD11c^{+}CD8^{-}$ and $B220^{-}CD11c^{+}CD8^{+}$) from $Cre^{CD11c}Casp8^{fl/fl}$ mice showed deletion of caspase-8, but this was not the case for plasmacytoid DCs ($CD11c^{int}PDCA-1^{+}B220^{+}$), lymphocytes, and macrophages (Supplemental Fig. 1). $Cre^{CD11c}Casp8^{fl/fl}$ bone marrow-derived DCs (BMDCs) showed caspase-8 deletion (Supplemental Fig. 1). $OT-II/RAG^{-/-}$ and $B6.CD45.1$ mice were purchased from The Jackson Laboratory. $RIPK3^{-/-}$ mice (Genentech), $IRF3^{-/-}$ mice (a gift from Mike Diamond, Washington University, St. Louis, MO), $IRF7^{-/-}$ mice (a gift from Mike Diamond), and $MyD88^{fl/fl}$ mice (The Jackson Laboratory) were bred to $Cre^{CD11c}Casp8^{fl/fl}$ mice, generating $RIPK3^{-/-}Cre^{CD11c}Casp8^{fl/fl}$, $IRF3^{-/-}Cre^{CD11c}Casp8^{fl/fl}$, $IRF7^{-/-}Cre^{CD11c}Casp8^{fl/fl}$, and $MyD88^{fl/fl}Cre^{CD11c}Casp8^{fl/fl}$ mice. Real-time PCR performed by Transnetyx on FACS-sorted splenic conventional DC populations from $MyD88^{fl/fl}Cre^{CD11c}Casp8^{fl/fl}$ mice showed caspase-8 and MyD88 deletion (Supplemental Fig. 1). Female mice were used in all studies. Proteinuria was assessed using Uristix (Siemens). Transnetyx performed genotyping. Experiments were approved by Northwestern University's Institutional Animal Care and Use Committee.

Histopathologic studies

Paraffin-embedded kidney sections (4 μ m) were stained with periodic acid–Schiff (PAS), and a pathologist blinded to the study scored kidney sections using an Olympus BS40 microscope, as previously described (22). Frozen kidney sections (4 μ m) were stained with anti-IgG–FITC (22). All images were photographed at $\times 40$, $\times 200$, or $\times 400$ magnification using an Olympus BX41 microscope equipped with an Olympus DP20 camera.

Flow cytometry

Surface staining of cell suspensions and gating strategies were accomplished as previously described (23, 24). At least 100,000 events were acquired on a BD LSR II instrument. Data were analyzed with FlowJo software (TreeStar). Dead cells were excluded using Aqua Live/Dead staining (Invitrogen). For cell-sorting studies, splenocytes preincubated with Fc-block were stained with fluorescent Abs (information available upon request). Splenocyte populations sorted on a BD FACSAria II instrument at the University of Chicago's Flow Core had an average purity of 97%.

Bone marrow chimeras

Bone marrow was aseptically harvested from tibias, femurs, and humeri from 9-wk-old mice, erythrocytes were lysed (BD Pharm Lyse buffer), and cells were incubated with Fc-block, followed by incubation with PE-conjugated Abs against B220, CD4, CD8, CD11b, Ly6G, NK1.1, Siglec F, and Ter119 (BD Biosciences and eBioscience). Cells were incubated with anti-PE MicroBeads (Miltenyi Biotec), and PE-labeled lineage cells were depleted (AutoMACS separator). Three-month-old $B6.CD45.1$ mice received a single 1000-cGy gamma radiation dose using a [^{137}Cs]-based

Gammacell 40 irradiator (Nordion). After 12 h, 1.2×10^6 lineage-depleted cells from $Casp8^{fl/fl}$ mice, $Cre^{CD11c}Casp8^{fl/fl}$ mice, $Casp8^{fl/fl}$ and $B6.CD45.1/2$ mice (1:1 ratio), or $Cre^{CD11c}Casp8^{fl/fl}$ and $B6.CD45.1/2$ mice (1:1 ratio) were injected i.v. Presorted cells were stained with c-Kit (eBioscience) and Sca-1 (BioLegend) to analyze the LSK fraction. Chimeric mice were maintained on autoclaved water plus antibiotics (Trimetoprim/sulfamethoxazole; Hi-Tech Pharmacal) for 4 wk after transfer and were phenotyped 18 wk after transfer.

In vivo assays

For TLR ligand-injection studies, 3-mo-old mice were injected i.p. with LPS, imiquimod, or CpG (200 μ g/20 g body weight; InvivoGen) and analyzed 4 h later by flow cytometry. For oral antibiotic treatment, 3-wk-old mice were given autoclaved water with ampicillin (1 g/l), vancomycin (0.5 g/l), neomycin sulfate (1 g/l), metronidazole (1 g/l), and sucrose (10 g/l) twice a week for 8 wk, with no observable weight loss. For BrdU assays, mice were injected i.v. with 1 mg BrdU (BD Biosciences) for 3 d. On days 0, 1, and 3 postinjection, splenocyte and bone marrow suspensions were prepared as described above. After surface staining, cells were processed with BrdU staining kits (BD Biosciences), according to the manufacturer's instructions. Fluorescence minus one controls were used to set gates for $BrdU^{+}$ populations.

In vitro assays

For MLRs, splenocytes were incubated with anti-CD19 beads, and negative fractions were incubated with anti-CD11c MACS beads (Miltenyi Biotec) to purify APCs. Purified APCs were pulsed with 10 μ g/ml OVA peptide (aa 323–339) for 60 min at 37°C. OVA-specific splenic $CD4^{+}$ T cells were isolated from $B6.CD45.1/OT-II/RAG^{-/-}$ mice using a $CD4^{+}$ T Cell Isolation Kit (Miltenyi Biotec), according to the manufacturer's instructions. Purity of APCs and T cells was 90%. T cells were labeled with CFSE (500 nM for 12 min at 37°C; Invitrogen). Pulsed APCs at various ratios were incubated with 2×10^5 CFSE-labeled T cells, with or without 5 μ g/ml CpG-B (ODN 1668), in triplicate in 96-well flat-bottom plates at 37°C for 3 d. Cell clusters were dissociated with 7.5 mM EDTA for 15 min and stained with anti-CD4 (BD Biosciences). 7-Aminoactinomycin D (0.25 mg/test; BD Biosciences) was used to exclude dead cells. A constant number of CaliBRITE beads (BD Biosciences) was added for acquisition of equal parts/culture. Live T cells were gated, and the number of divided cells showing less than maximal CFSE fluorescence intensity was determined. For cell death assays, bead-sorted $CD4^{+}$ T cells were incubated with anti-CD3 (0.5 μ g/ml) and anti-CD28 (1 μ g/ml; both from BD Biosciences), with or without zVAD-FMK (20 μ M; Promega) and necrostatin-1 (30 μ M; Enzo Life Sciences), and stained with Annexin V (Invitrogen) and Aqua Live/Dead 72 h later, according to the manufacturer's instructions.

BMDCs were generated as described (25). Briefly, bone marrow was resuspended in complete media with 50 μ M 2-ME and cultured for 2 h. A total of 1×10^6 nonadherent cells was placed in 24-well plates containing 1 ml complete media plus GM-CSF (10 ng/ml) and Flt3-L (50 ng/ml; both from PeproTech). Two thirds of the media was replaced on day 3. On days 5 and 7, nonadherent cells were transferred into six-well plates in media plus cytokines (2.5×10^6 cells/2 ml/well) for 2 d, and BMDCs were used on day 9 at a concentration of 1.75×10^6 /ml. Supernatants and nuclear lysates from BMDCs that were stimulated for 6 h at 37°C in 5% CO_2 with LPS (10 ng/ml; Sigma-Aldrich), CpG (5 μ g/ml), and imiquimod (5 μ g/ml) were evaluated for cytokine levels and transcription factor binding, respectively (see below). Total cell lysates from BMDCs that were stimulated for 30 or 60 min at 37°C in 5% CO_2 with imiquimod (5 μ g/ml) were evaluated for transcription factor expression levels. BMDCs also were stimulated for 6 h at 37°C in 5% CO_2 with LPS (10 ng/ml), CpG (5 μ g/ml), and imiquimod (5 μ g/ml), with or without necrostatin-1 (30 μ M), and/or zETD-FMK (20 μ M; BD Biosciences), and/or 1-methyl-D-tryptophan (30 μ M; Sigma-Aldrich), and supernatants were evaluated for cytokine levels. ATP (5 mM; Sigma-Aldrich) was added for 30 min and then media were replaced for an additional hour to evaluate IL-1 β levels. For cell death assays, 3×10^6 BMDCs or total splenocytes were stimulated for 10 h at 37°C in 5% CO_2 with SuperFasLigand (100 ng/ml; Enzo Life Sciences) or etoposide (10 μ M; Alexis Biochemicals), with or without necrostatin-1 (30 μ M), and then stained with Annexin V and Aqua Live/Dead.

Ab/cytokine measurements and transcription factor binding and expression quantification

Anti-nuclear Abs, including anti-dsDNA, anti-ssDNA, or anti-chromatin, were measured as previously described (22). Total IgM and IgG isotypes

and cytokine/chemokine expression were quantified using Luminex-based assays (Affymetrix). Transcription factor analysis was accomplished using Nuclear Extraction and Procarta TF Plex Kits, according to the manufacturer's instructions (Affymetrix). Immunoblot analysis was performed as previously described (26), and the concentrations of the primary Abs were as follows: 1:1000 for rabbit anti-IRF3 Ab (Cell Signaling), 1 mg/ml for rabbit anti-IRF7 Ab (Abcam), and 1:500 for mouse anti-GAPDH Ab (US Biological).

Statistical analysis

GraphPad Prism 5.0 software was used for statistical analyses. Data are mean ± SD and were compared using the Mann–Whitney *U* test, unless otherwise noted.

Results

Mice with conditional deletion of caspase-8 in DCs develop a chronic systemic autoimmune disease

We examined the consequences of DC-specific deletion of caspase-8 (*Cre^{CD11c}Casp8^{fl/fl}*). Loss of caspase-8 in DCs led to splenomegaly and lymphadenopathy in young (Supplemental Fig. 2A, 2B) and aged (Fig. 1A–C) mice. However, the observed splenomegaly in aged *Cre^{CD11c}Casp8^{fl/fl}* mice was not attributed to the increased numbers of splenocytes (Fig. 1D) or CD45⁺ cells or Ter119⁺ cells (Supplemental Fig. 2C, 2D). Additionally, there was a disruption of the splenic architecture in *Cre^{CD11c}Casp8^{fl/fl}* mice compared

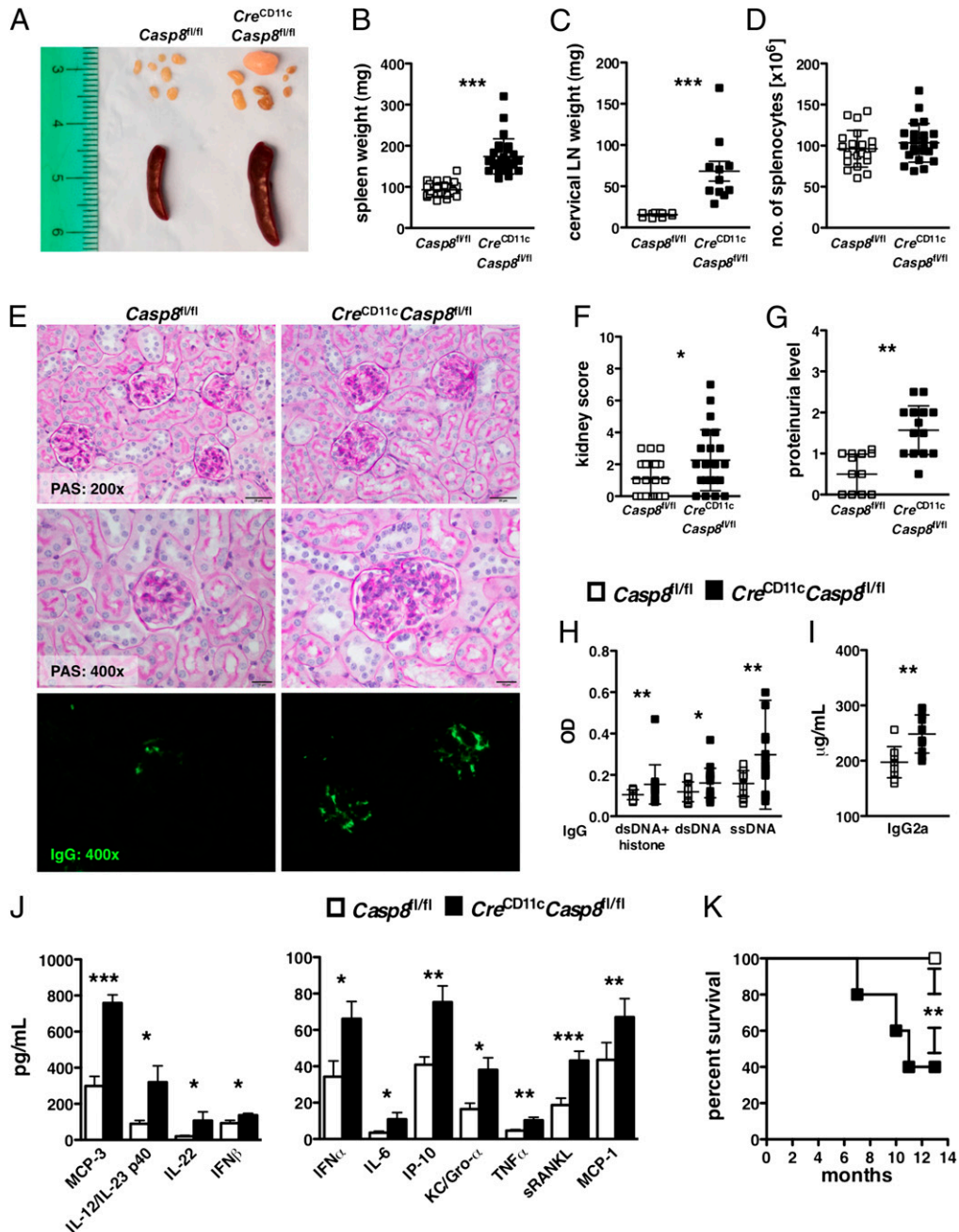


FIGURE 1. Mice with DC-specific deletion of caspase-8 exhibit systemic autoimmunity. (A–J) Eight-month-old female *Casp8^{fl/fl}* (control) and *Cre^{CD11c}Casp8^{fl/fl}* mice ($n \geq 10$) were evaluated for systemic autoimmune disease phenotypes. (A) Representative spleens and lymph nodes. (B) Splenomegaly. (C) Lymphadenopathy. (D) Number of splenocytes. (E) PAS-stained formalin-fixed kidney sections and anti-IgG-FITC-stained frozen kidney sections. (F) Kidney score. (G) Proteinuria. Serum levels of chromatin-, dsDNA-, and ssDNA-reactive IgG Abs (H), pathogenic IgG2a Abs (I), and cytokines and chemokines (J). Data are mean ± SD. * $p < 0.05$, ** $p < 0.005$, *** $p < 0.0005$, Mann–Whitney *U* test. (K) Survival curve. ** $p < 0.005$, log-rank Mantel–Cox test.

with control mice, as shown by the expansion of white pulp and reduction of red pulp (Supplemental Fig. 2E). There also was a slight increase in splenic collagen deposition in $Cre^{CD11c}Casp8^{fl/fl}$ mice compared with control mice and no detectable liver pathology (Supplemental Fig. 2E). $Cre^{CD11c}Casp8^{fl/fl}$ mice developed glomerulonephritis (Fig. 1E, 1F), IgG deposition in the kidney (Fig. 1E), and proteinuria compared with control mice (Fig. 1G). $Cre^{CD11c}Casp8^{fl/fl}$ mice exhibited markedly elevated levels of serum chromatin-, dsDNA-, and ssDNA-reactive IgG Abs (Fig. 1H), pathogenic IgG2a Abs (Fig. 1I), and proinflammatory cytokines and chemokines, including MCP-3, IL-12/IL-23p40, IL-22, IFN- β , IFN- α , IL-6, IP-10, KC/Gro- α , TNF- α , soluble RANKL, and MCP-1 (Fig. 1J), compared with control

mice. $Cre^{CD11c}Casp8^{fl/fl}$ mice also exhibited spontaneous early mortality beginning at 7 mo of age; 50% of the mice died by 11 mo of age (Fig. 1K).

Inflammation is independent of DC survival in DC-specific caspase-8-deficient mice

Stimulation with FasL had a minimal effect on the survival of BMDCs (Fig. 2A) and splenic DCs (Fig. 2B), regardless of the presence of caspase-8, consistent with previous studies (27, 28). Splenic T cells from control and DC-specific caspase-8-deficient mice displayed similar levels of FasL-induced death (Fig. 2C) and etoposide-induced death (Fig. 2D). Consistent with recent studies (29), necrostatin-1, an inhibitor of RIPK1 kinase activity and

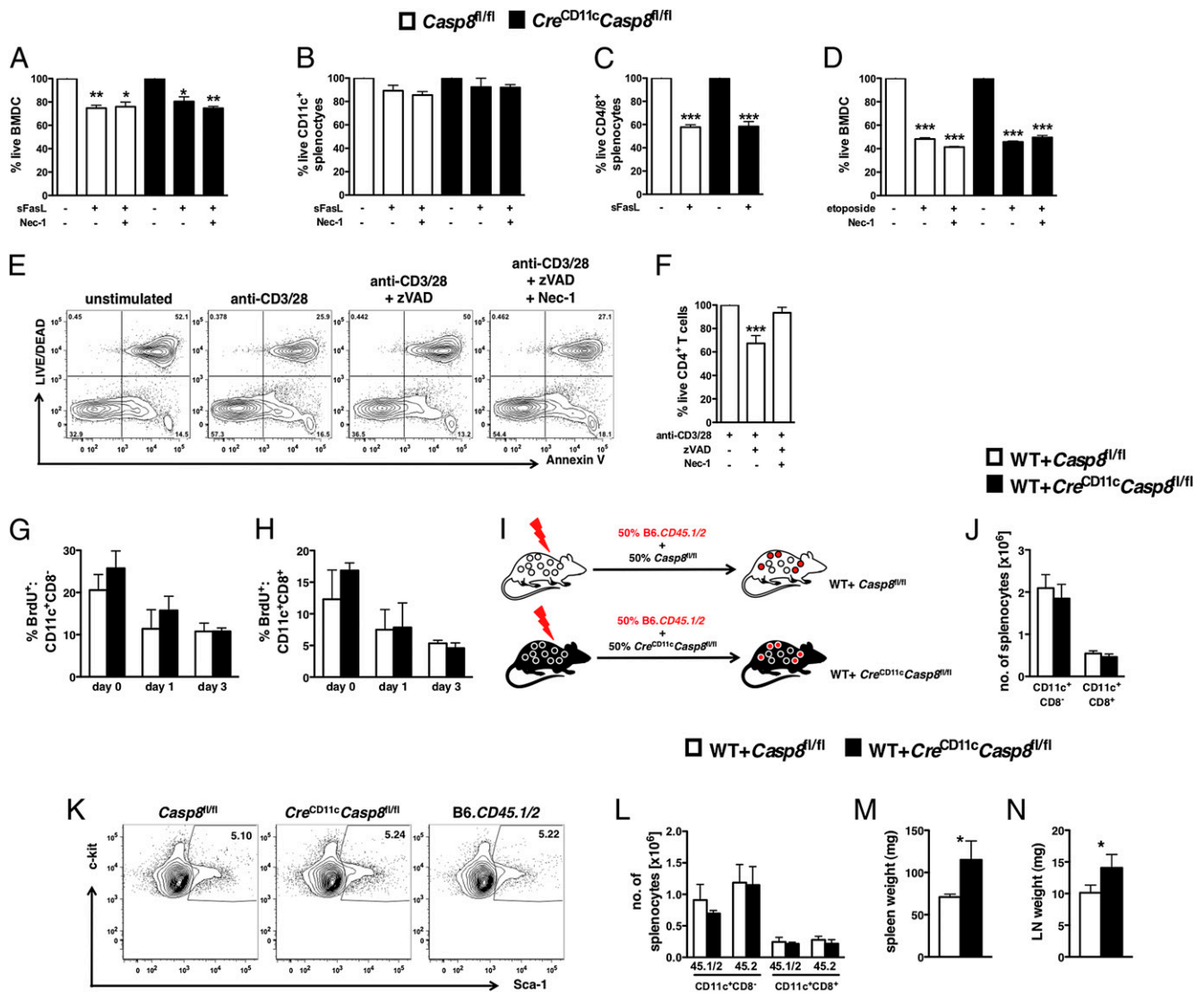


FIGURE 2. Inflammation related to DC-specific caspase-8 deficiency is independent of DC survival. $Casp8^{fl/fl}$ (control) and $Cre^{CD11c}Casp8^{fl/fl}$ BMDCs ($n = 4$) (A) and total splenocytes ($n = 3$) (B and C) were stimulated with SuperFasL (sFasL), with or without necrostatin-1 (Nec-1), for 10 h and stained with Annexin V and Aqua Live/Dead. Total splenocytes were gated into CD11c⁺ (B) and CD4⁺ (C) populations for analysis. (D) Additionally, control and $Cre^{CD11c}Casp8^{fl/fl}$ BMDCs were stimulated with etoposide for 10 h and stained with Annexin V and Aqua Live/Dead. Data are the percentage of live divided by the unstimulated condition. (E and F) CD4⁺ T cells ($n = 3$), stimulated for 72 h with anti-CD3 and anti-CD28, with or without pan-caspase inhibitor zVAD-FMK (zVAD) and Nec-1, were stained with Annexin V and Aqua Live/Dead. Data are the percentage of live divided by the anti-CD3/28 condition. Control and $Cre^{CD11c}Casp8^{fl/fl}$ mice ($n = 4$), injected with BrdU for 3 d (G and H), were evaluated for the percentage of splenic BrdU⁺ CD11c⁺ CD8⁻ (L) and CD11c⁺CD8⁺ (M) conventional DCs. (I–M) Mice were reconstituted with equal portions of B6.CD45.1/2 (WT) and either control or $Cre^{CD11c}Casp8^{fl/fl}$ bone marrow ($n = 5$). (I) Representation of experimental design. (J) Representative Lin⁻ Sca-1⁻c-kit⁺ bone marrow cell percentages from 3-mo-old female control, $Cre^{CD11c}Casp8^{fl/fl}$, and WT mice. Chimeric mice were evaluated 3 mo after transfer for numbers of conventional DCs (K), distribution of WT (45.1/2) and control or $Cre^{CD11c}Casp8^{fl/fl}$ (45.2) derived conventional DCs (L), splenomegaly (M), and lymphadenopathy (N). Data are mean \pm SD. * $p < 0.05$, ** $p < 0.005$, *** $p < 0.0005$, Mann–Whitney U test.

necroptosis, had no effect on the viability of DCs (Fig. 2A, 2B, 2D), but it rescued activated T cells cultured with the pan-caspase inhibitor zVAD-FMK (Fig. 2E, 2F).

Previous studies evaluating mice lacking Fas in DCs or overexpressing the p35 caspase inhibitor suggested a link between an autoimmune disease phenotype and deficiency in DC apoptosis (14, 20). Because caspase-8 is a downstream signaling component of Fas, and p35 inhibits all caspase activity, DC survival was examined using *in vivo* BrdU pulse chase assays and mixed chimeras. BrdU pulse chase assays showed no difference in DC turnover rates between $Cre^{CD11c}Casp8^{fl/fl}$ and control conventional DCs (Fig. 2G, 2H). Additionally, loss of caspase-8 in DCs did not result in enhanced survival, because splenic conventional DC numbers remained unchanged in mixed chimera mice (wild-type [WT]+ $Cre^{CD11c}Casp8^{fl/fl}$, Fig. 2I, 2J). Of note, the transferred LSK population ($Lin^{-}Sca-1^{+}c-kit^{+}$) was similar in $Cre^{CD11c}Casp8^{fl/fl}$, $Casp8^{fl/fl}$, and WT mice (Fig. 2K). Further, there was no survival advantage attributed to the loss of caspase-8 in DCs, because there were no differences in the number of $Cre^{CD11c}Casp8^{fl/fl}$ and WT-derived splenic conventional DCs in mixed chimera mice (Fig. 2L), consistent with parallel DC turnover rates in BrdU pulse chase assays. In contrast, hallmarks of systemic autoimmunity, including splenomegaly (Fig. 2M) and lymphadenopathy (Fig. 2N), persisted in mixed chimera mice.

RIPK3 knockout fails to reverse the consequences of DC-specific caspase-8 deletion

Because RIPK3 knockout reverses the phenotype in global and T cell–specific caspase-8–deficient mice (18, 19), we crossed $Cre^{CD11c}Casp8^{fl/fl}$ mice to $RIPK3^{-/-}$ mice. Young $RIPK3^{-/-}Cre^{CD11c}Casp8^{fl/fl}$ mice developed splenomegaly (Supplemental Fig. 2A), but lymphadenopathy was abated compared with $Cre^{CD11c}Casp8^{fl/fl}$ mice (Supplemental Fig. 2B). However with age, $RIPK3^{-/-}Cre^{CD11c}Casp8^{fl/fl}$ mice exhibited splenomegaly and lymphadenopathy at unchanged and exacerbated levels, respectively, compared with $Cre^{CD11c}Casp8^{fl/fl}$ mice (Fig. 3A–C). $RIPK3^{-/-}Cre^{CD11c}Casp8^{fl/fl}$ mice also presented with glomerulonephritis (Fig. 3D, 3E) and IgG deposition in the kidney (Fig. 3D), although proteinuria was reduced compared with $Cre^{CD11c}Casp8^{fl/fl}$ mice (Fig. 3F). Further, although serum levels of chromatin-reactive, dsDNA-reactive, and ssDNA-reactive IgG Ab levels (Fig. 3G) were unaffected by the additional loss of RIPK3, pathogenic IgG2a Abs (Fig. 3H) and proinflammatory molecules IL-22, IL-6, and sRANKL (Fig. 3I) were heightened compared with $Cre^{CD11c}Casp8^{fl/fl}$ mice. Moreover, $Cre^{CD11c}Casp8^{fl/fl}$ mice did not present with the characteristic double-negative T cell population ($CD4^{-}CD8^{-}CD3^{+}B220^{+}$) associated with deficiencies in Fas (30). In contrast, $RIPK3^{-/-}Cre^{CD11c}Casp8^{fl/fl}$ mice developed a double-negative T cell population in a similar proportion to B6.*lpr* mice (Supplemental Fig. 2F–I).

Deletion of IRF3 exacerbates the systemic inflammation in $Cre^{CD11c}Casp8^{fl/fl}$ mice

$Cre^{CD11c}Casp8^{fl/fl}$ mice present with an IFN signature, indicating that the loss of caspase-8 may increase the activity of IRFs, a family of transcription factors known to play a role in type 1 IFN production. Caspase-8–deficient BMDCs showed sustained DNA binding of IRF in response to treatment with CpG (TLR9 agonist), imiquimod (TLR7 agonist), and LPS (TLR4 agonist). Moreover, STAT1 and IRF signaling response elements exhibited increased DNA binding following TLR7 and TLR4 stimulation in caspase-8–deficient BMDCs (Fig. 4A), with no difference in the DNA binding activity of NF- κ B between control and $Cre^{CD11c}Casp8^{fl/fl}$ BMDCs. Further, because previous studies showed that caspase-

processes IRF3 for degradation (13), examination of caspase-8–deficient BMDCs revealed constitutively higher expression of IRF3, as well as IRF7, compared with control BMDCs and independent of TLR stimulation (Fig. 4B). Therefore, we generated $IRF3^{-/-}Cre^{CD11c}Casp8^{fl/fl}$ mice to determine the role of IRF3 in the induction of systemic inflammation. Because IRF7 is a redundant homolog of IRF3, we established $IRF7^{-/-}Cre^{CD11c}Casp8^{fl/fl}$ mice as a control. Interestingly, knockout of IRF3 exacerbated the splenomegaly and lymphadenopathy in both young (Supplemental Fig. 2A, 2B) and aged (Fig. 4C–E) $Cre^{CD11c}Casp8^{fl/fl}$ mice, whereas IRF7 knockout had no additive effect. Although loss of IRF3 or IRF7 did not dramatically affect the presence of glomerulonephritis (Fig. 4F, 4G), IgG deposition in the kidney (Fig. 4F), or proteinuria (Fig. 4H) in $Cre^{CD11c}Casp8^{fl/fl}$ mice, $IRF3^{-/-}Cre^{CD11c}Casp8^{fl/fl}$ mice, but not $IRF7^{-/-}Cre^{CD11c}Casp8^{fl/fl}$ mice, exhibited markedly elevated levels of serum chromatin– and dsDNA-reactive IgG Abs (Fig. 4I), pathogenic IgG2a Abs (Fig. 4J), and proinflammatory molecules, including IL-6, TNF- α , and sRANKL (Fig. 4K), compared with $Cre^{CD11c}Casp8^{fl/fl}$ mice.

Caspase-8–deficient DCs are hyperresponsive to TLR activation

Because of the chronic systemic inflammation observed in $Cre^{CD11c}Casp8^{fl/fl}$ mice regardless of the presence of RIPK3, we assessed the response to TLR agonists in the absence of caspase-8. Of note, expression of TLR2/4/7/9 was either unchanged or reduced in $Cre^{CD11c}Casp8^{fl/fl}$ splenic DC subsets compared with controls (Supplemental Fig. 3A). To determine the functional response of these TLRs in caspase-8–deficient DCs, BMDCs were treated with CpG, imiquimod, or LPS. $Cre^{CD11c}Casp8^{fl/fl}$ BMDCs produced higher levels of IL-12/23p40, IL-6, TNF- α , and IL-1 β compared with control BMDCs in response to TLR7 (Fig. 5A), TLR9, and TLR4 activation (Supplemental Fig. 3B) without inducing cell death (Supplemental Fig. 3C). The loss of caspase-8 was sufficient to induce IL-1 β release without the addition of ATP (Supplemental Fig. 3D). To expand upon these studies, the aforementioned TLR agonists were injected *i.p.* into mice. Although CpG and LPS had no effect on expression of activation markers in $Cre^{CD11c}Casp8^{fl/fl}$ mice (data not shown), imiquimod induced a large increase in CD86 expression and led to elevated MHC class II and CD40 expression on $Cre^{CD11c}Casp8^{fl/fl}CD11c^{+}CD8^{-}$ conventional DCs compared with controls (Fig. 5B, 5C).

Although DCs do not undergo necroptosis, we examined whether the necrosome has an effect on proinflammatory cytokine production. Necrostatin-1 inhibited secretion of IL-6, TNF- α , and IL-1 β in all TLR agonist–treated caspase-8–deficient BMDC cultures, whereas it only reduced IL-12/23p40 secretion mediated by TLR9 activation (Fig. 5A, Supplemental Fig. 3B). Because necrostatin-1 was shown to block RIPK1, as well as IDO, the IDO2-specific inhibitor 1-methyl-D-tryptophan (1-MT) (31) was added to BMDC cultures as a control. 1-MT had no effect on cytokine secretion, with the exception of CpG-induced IL-12/23p40 production in BMDCs. The caspase-8–specific inhibitor zIETD-FMK also was added to BMDCs to address the requirement for caspase-8 enzymatic activity in the hypersecretion of proinflammatory cytokines. Interestingly, specific blockade of caspase-8 activity did not mimic the deletion of caspase-8 in BMDCs (Fig. 5A, Supplemental Fig. 3B).

Caspase-8 suppresses MyD88 signaling

Over the past several years, gut microflora have been suggested to be a depot for TLR signaling (32). To reduce the potential for

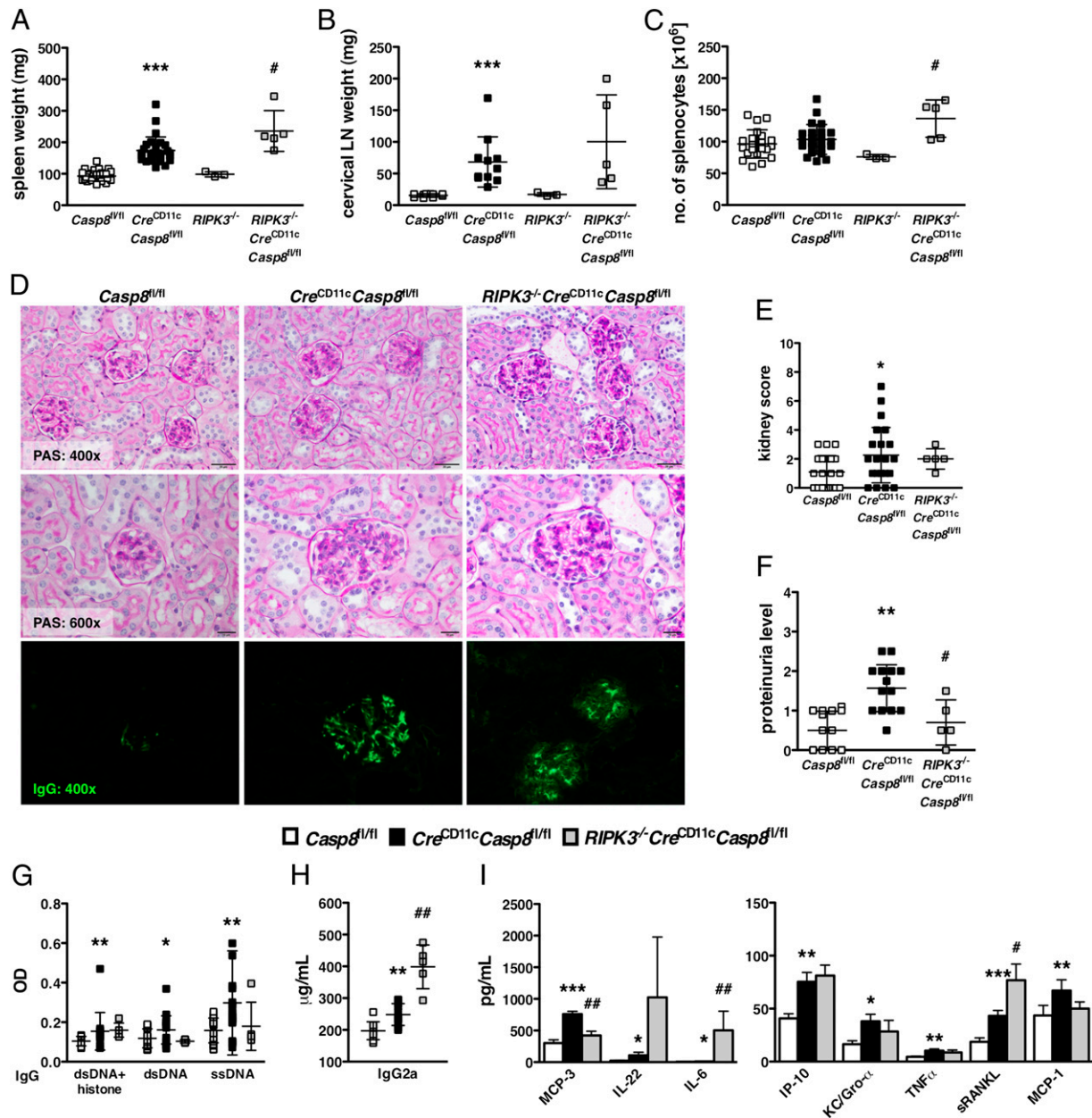


FIGURE 3. RIPK3 knockout cannot reverse the consequences of DC-specific caspase-8 deletion. (A–I) Six-month-old female *Casp8^{fl/fl}* (control), *Cre^{CD11c}Casp8^{fl/fl}*, and *RIPK3^{-/-}Cre^{CD11c}Casp8^{fl/fl}* mice ($n \geq 5$) were evaluated for systemic autoimmune disease phenotypes. (A) Splenomegaly. (B) Lymphadenopathy. (C) Number of splenocytes. (D) PAS-stained formalin-fixed kidney sections and anti-IgG–FITC–stained frozen kidney sections. (E) Kidney score. (F) Proteinuria. Serum was evaluated for levels of chromatin-, dsDNA-, and ssDNA-reactive IgG Abs (G), pathogenic IgG2a Abs (H), and cytokines and chemokines (I). Data are mean \pm SD. * $p < 0.05$, ** $p < 0.005$, *** $p < 0.0005$, control versus *Cre^{CD11c}Casp8^{fl/fl}*, Mann–Whitney U test. # $p < 0.05$, ## $p < 0.005$, *Cre^{CD11c}Casp8^{fl/fl}* versus *RIPK3^{-/-}Cre^{CD11c}Casp8^{fl/fl}*, Mann–Whitney U test.

endogenous TLR ligands from gut microflora to exacerbate SLE-like disease, young *Cre^{CD11c}Casp8^{fl/fl}* mice were treated with oral antibiotics for 2 mo. Oral antibiotic treatment had no effect on disease development in *Cre^{CD11c}Casp8^{fl/fl}* mice, because splenomegaly (Fig. 6A) and lymphadenopathy (Fig. 6B) were unchanged compared with untreated *Cre^{CD11c}Casp8^{fl/fl}* mice.

Because of the heightened production of proinflammatory cytokines associated with caspase-8 deficiency, we sought to restrict TLR activation in our model by eliminating MyD88. Concurrent deletion of caspase-8 and MyD88 in DCs was sufficient to reduce splenomegaly and lymphadenopathy in aged *Cre^{CD11c}Casp8^{fl/fl}* mice (Fig. 6C, 6D), but it did not affect splenocyte numbers (Fig. 6E). Importantly, loss of MyD88 ameliorated kidney disease observed in *Cre^{CD11c}Casp8^{fl/fl}* mice, as shown by reduced glomerulonephritis (Fig. 6F, 6G) and IgG deposition (Fig. 6F), although proteinuria levels (Fig. 6H) were unchanged. Further, although *MyD88^{fl/fl}Cre^{CD11c}Casp8^{fl/fl}* mice exhibited similar levels of chromatin- and dsDNA-reactive IgG Abs (Fig. 6I) and pathogenic IgG2a Abs (Fig. 6J), there was a trend toward reduced ssDNA-reactive IgG Abs (Fig. 6I) and significantly less proinflammatory serum cytokines/chemokines, including IL-22 and MCP-3 (Fig. 6K), compared with *Cre^{CD11c}Casp8^{fl/fl}* mice.

DC-specific loss of caspase-8 intensifies DC and lymphocyte activation

To determine the cellular mechanism responsible for the systemic autoimmunity that develops in *Cre^{CD11c}Casp8^{fl/fl}* mice, multiparameter flow cytometry was used. *Cre^{CD11c}Casp8^{fl/fl}* CD4⁺ T cells,

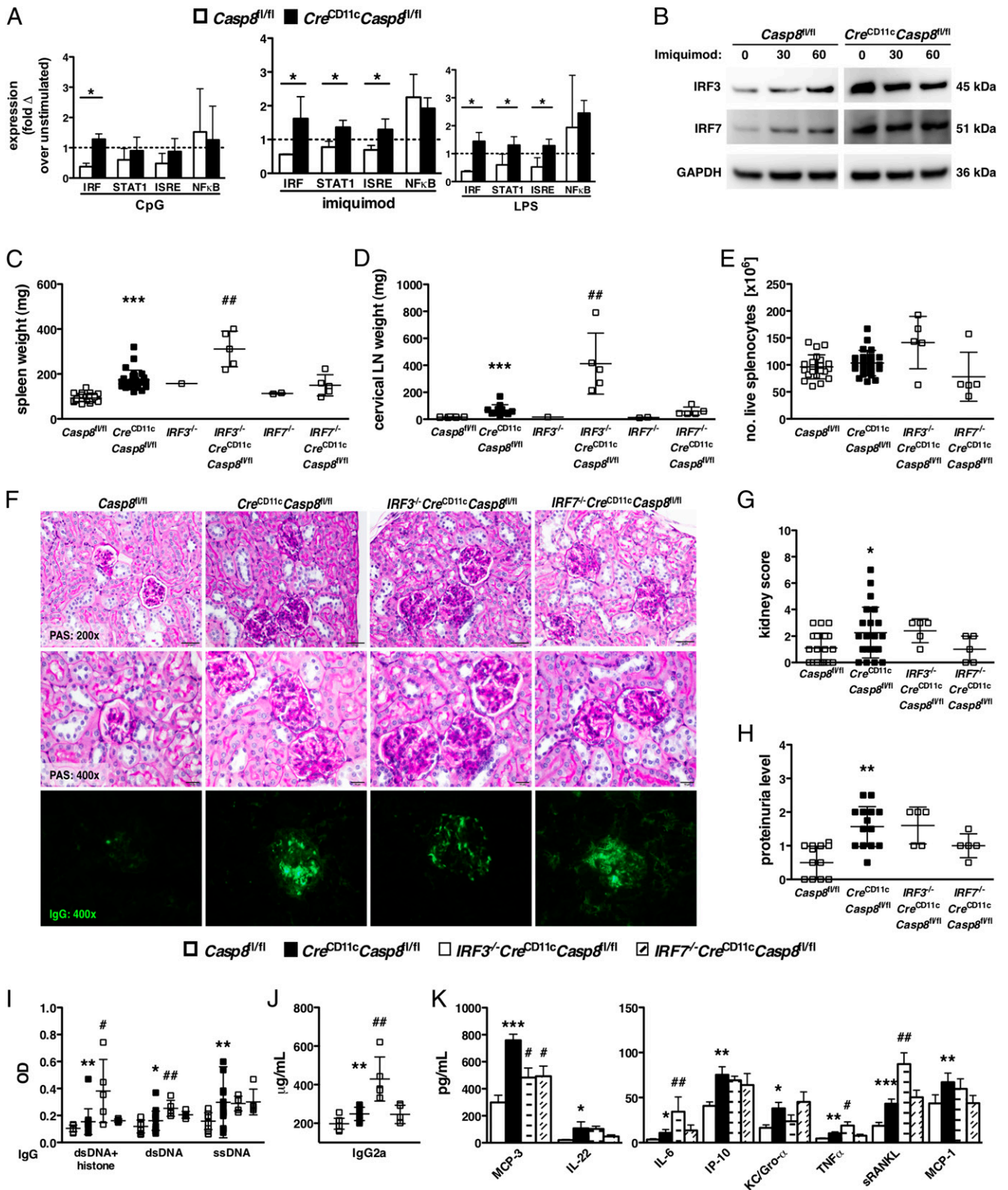


FIGURE 4. Deletion of IRF3 exacerbates the systemic inflammation in *Cre^{CD11c}Casp8^{fl/fl}* mice. **(A)** *Casp8^{fl/fl}* (control) and *Cre^{CD11c}Casp8^{fl/fl}* BMDCs were stimulated with CpG, imiquimod, or LPS for 6 h, and isolated nuclear lysates were subjected to a multianalyte transcription factor bead-based assay. Data are represented as the fold change over unstimulated cells. **(B)** Control and *Cre^{CD11c}Casp8^{fl/fl}* BMDCs were stimulated with imiquimod, and isolated total cellular lysates were subjected to immunoblot analysis for total IRF3. The blot was then stripped for total IRF7 and GAPDH expression, and the figures were cropped and pieced together. **(C–K)** Seven-month-old female *Casp8^{fl/fl}* (control), *Cre^{CD11c}Casp8^{fl/fl}*, *IRF3^{-/-}Cre^{CD11c}Casp8^{fl/fl}*, and *IRF7^{-/-}Cre^{CD11c}Casp8^{fl/fl}* mice ($n \geq 5$) were evaluated for systemic autoimmune disease phenotypes. **(C)** Splenomegaly. **(D)** Lymphadenopathy. **(E)** Number of splenocytes. **(F)** PAS-stained formalin-fixed kidney sections and anti-IgG-FITC-stained frozen kidney sections. **(G)** Kidney score. **(H)** Proteinuria. Serum was evaluated for levels of chromatin-, dsDNA-, and ssDNA-reactive IgG Abs **(I)**, pathogenic IgG2a Abs **(J)**, and cytokines and chemokines **(K)**. Data are mean \pm SD. * $p < 0.05$, ** $p < 0.005$, *** $p < 0.0005$, control versus *Cre^{CD11c}Casp8^{fl/fl}*, Mann-Whitney *U* test. # $p < 0.05$, ## $p < 0.005$, *Cre^{CD11c}Casp8^{fl/fl}* versus *IRF3^{-/-}Cre^{CD11c}Casp8^{fl/fl}* or *IRF7^{-/-}Cre^{CD11c}Casp8^{fl/fl}*, Mann-Whitney *U* test.

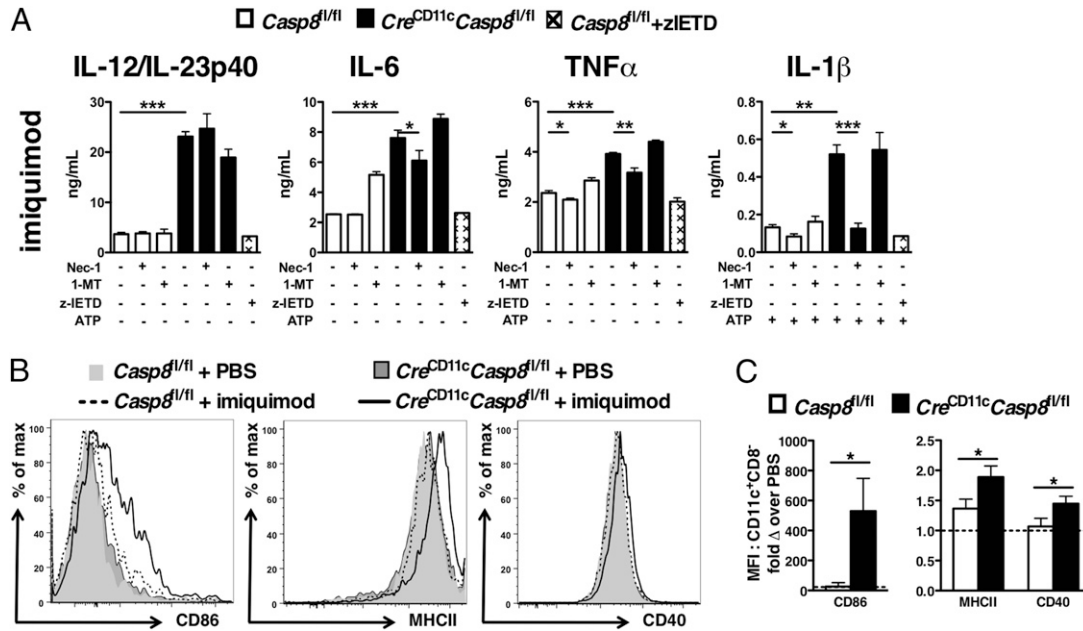


FIGURE 5. Caspase-8-deficient DCs are hyperresponsive to TLR activation in a RIPK1-dependent manner. **(A)** GM-CSF + Flt3-L-treated BMDCs from *Casp8^{fl/fl}* (control) and *Cre^{CD11c}Casp8^{fl/fl}* mice were stimulated with imiquimod, with or without Nec-1, zIETD-FMK (zIETD), or 1-MT for 6 h, with or without ATP (5 mM), and supernatants were evaluated for IL-12/IL-23p40, IL-6, TNF- α , and IL-1 β . **(B and C)** Three-month-old control and *Cre^{CD11c}Casp8^{fl/fl}* mice ($n = 4$) were injected with imiquimod (200 μ g/mouse) or PBS and evaluated 4 h later for splenic CD11c⁺CD8⁻ conventional DC CD86, MHCII, and CD40 expression. Data are the fold change over PBS injection. Data are mean \pm SD. * $p < 0.05$, ** $p < 0.005$, *** $p < 0.0005$, Mann-Whitney U test.

but not CD8⁺ T cells, were increased in numbers (Fig. 7A, 7B). Further, both CD4 and CD8 T cell populations showed decreased naive (CD44⁻CD62L⁺) and increased effector (CD44⁺CD62L⁻) subsets compared with controls (Fig. 7C, Supplemental Fig. 4A, 4B). Elevated expression of PD-1 on CD4⁺ T cells and CD69 and PD-1 on CD8⁺ T cells in *Cre^{CD11c}Casp8^{fl/fl}* mice further defined hyperactive T cell subsets (Supplemental Fig. 4C–F). Regulatory T cells (CD4⁺CD25⁺Foxp3⁺) were present at greater numbers in *Cre^{CD11c}Casp8^{fl/fl}* mice, and these cells expressed elevated PD-1 (Supplemental Fig. 4G, 4H). Although the loss of caspase-8 in DCs did not affect total B cell numbers (Fig. 7D), *Cre^{CD11c}Casp8^{fl/fl}* mice displayed an increase in marginal zone (MZ) B cells. *Cre^{CD11c}Casp8^{fl/fl}* total B cells expressed less IgD, indicating increased maturation and class-switching, and expressed more CD80, CD86, and PD-1 (Fig. 7E, Supplemental Fig. 4I–L), which correlates with the elevated Ab and autoantibody production observed in *Cre^{CD11c}Casp8^{fl/fl}* mice.

Because T and B cell activation is associated with DC functionality, *Cre^{CD11c}Casp8^{fl/fl}* DC populations were evaluated. *Cre^{CD11c}Casp8^{fl/fl}* mice showed more splenic CD11c⁺CD8⁻ conventional DCs and less CD11c⁺CD8⁺ conventional and plasmacytoid DCs compared with control mice (Fig. 7F). Further, both *Cre^{CD11c}Casp8^{fl/fl}* CD11c⁺CD8⁻ conventional and plasmacytoid DCs were hyperactivated (Fig. 7G, Supplemental Fig. 4M), as indicated by increased expression of costimulatory molecules CD80 and CD86 and activation marker CD69, respectively. Similar to DC subsets, *Cre^{CD11c}Casp8^{fl/fl}* mice exhibited increased numbers of Ly6C^{low} and Ly6C^{high} splenic monocytes/macrophages and neutrophils compared with control mice (Supplemental Fig. 4M). In addition, caspase-8-deficient CD11c⁺ cells incubated with OVA-peptide induced heightened OT-II-specific CD4⁺ T cell proliferation with and without TLR9 activation (Fig. 7H) as compared with control CD11c⁺ cells.

Knockout of RIPK3 or IRF3 not only exacerbated disease phenotypes, but also exaggerated the immune cell dysregulation

found in *Cre^{CD11c}Casp8^{fl/fl}* mice. Loss of RIPK3 increased the CD4⁺ (Fig. 7A) and regulatory (Supplemental Fig. 4G) T cell populations and heightened CD4⁺ and CD8⁺ T cell activation, as seen by increased skewing toward an effector phenotype (Figure 7C and Supplemental Fig. 4A, 4B) and elevated expression of CD69 on CD4⁺ T cells (Supplemental Fig. 4C) and PD-1 on CD4⁺, CD8⁺, and regulatory T cells (Supplemental Fig. 4D, 4F, 4H). RIPK3 deletion also modified B cells by reducing IgD levels (Fig. 7E, Supplemental Fig. 4I), indicating increased maturation, compared with caspase-8 deficiency alone. Systemic RIPK3 deletion increased DC numbers (Fig. 7F), and modified CD11c⁺CD8⁻ conventional DC activation by decreasing CD80 expression (Fig. 7G) to control levels while increasing CD86 expression (Fig. 7G). Although loss of IRF3 did not affect T cell numbers overall (Fig. 7A, 7B), effector T cells were increased while naive T cells were reduced compared with *Cre^{CD11c}Casp8^{fl/fl}* T cells (Fig. 7C, Supplemental Fig. 4A, 4B). Although IRF3 deletion increased neutrophil, eosinophil, and Ly6C^{low} and Ly6C^{high} splenic macrophage numbers (Supplemental Fig. 4N), DC numbers were unaffected (Fig. 7F). However, IRF3 deletion elevated CD11c⁺CD8⁻ conventional DC CD86 expression (Fig. 7G).

Although knockout of IRF7 did not affect disease phenotypes in found in *Cre^{CD11c}Casp8^{fl/fl}* mice, IRF7 deletion not only decreased numbers of CD4⁺ and CD8⁺ (Fig. 7A, 7B) T cells, and reduced expression of PD-1 on CD4⁺, CD8⁺ and regulatory T cells (Supplemental Fig. 4D, 4F, 4H), but also reduced CD11c⁺CD8⁻ conventional DC CD80 expression (Fig. 7G) in *Cre^{CD11c}Casp8^{fl/fl}* mice. However, these alterations at the cellular level were insufficient to reduce disease activity.

DC-specific deletion of MyD88 not only partially reversed the SLE-like disease phenotype in *Cre^{CD11c}Casp8^{fl/fl}* mice, but loss of this TLR signaling mediator also altered the observed immune cell dysregulation found in these mice. Although loss of MyD88 did not affect T cell numbers (Fig. 7A, 7B), CD8⁺ T cells expressed less CD69 (Supplemental Fig. 4E) and regulatory T cells

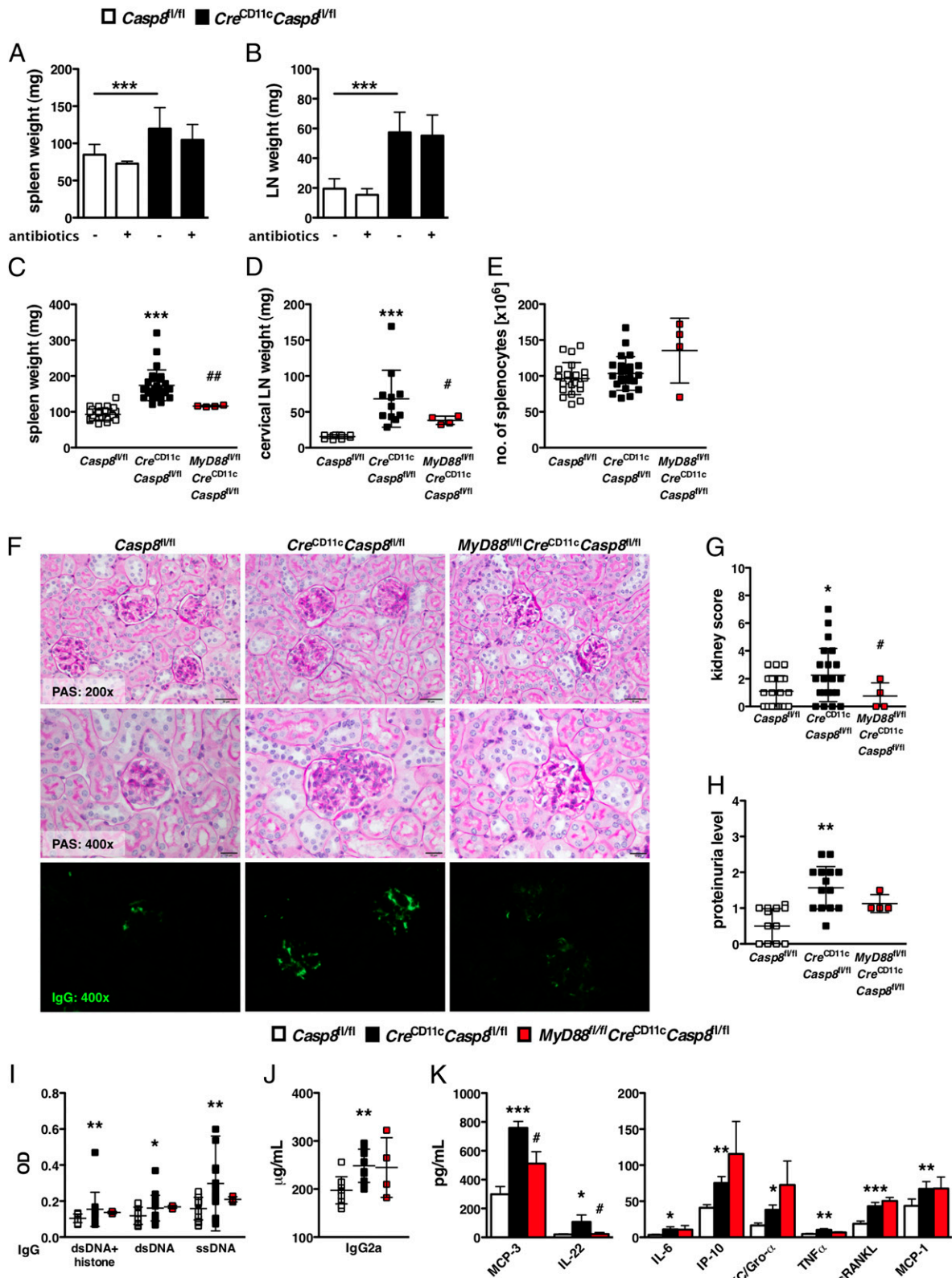


FIGURE 6. Caspase-8 suppresses MyD88 signaling. (**A** and **B**) Three-week-old *Casp8^{fl/fl}* (control) and *Cre^{CD11c}Casp8^{fl/fl}* ($n = 4$) mice were treated with oral antibiotics for 8 wk and evaluated for splenomegaly (**A**) and lymphadenopathy (**B**). (**C–K**) Eight-month-old female control, *Cre^{CD11c}Casp8^{fl/fl}*, and *MyD88^{fl/fl}Cre^{CD11c}Casp8^{fl/fl}* mice ($n \geq 4$) were evaluated for systemic autoimmune disease phenotypes. (**C**) Splenomegaly. (**D**) Lymphadenopathy. (**E**) Number of splenocytes. (**F**) PAS-stained formalin-fixed kidney sections and anti-IgG-FITC-stained frozen kidney sections. (**G**) Kidney score. (**H**) Proteinuria. Serum was evaluated for levels of chromatin-, dsDNA-, and ssDNA-reactive IgG Abs (**I**), pathogenic IgG2a Abs (**J**), and cytokines and chemokines (**K**). Data are mean \pm SD. * $p < 0.05$, ** $p < 0.005$, *** $p < 0.0005$, control versus *Cre^{CD11c}Casp8^{fl/fl}*, Mann-Whitney U test. # $p < 0.05$, ## $p < 0.005$, *Cre^{CD11c}Casp8^{fl/fl}* versus *MyD88^{fl/fl}Cre^{CD11c}Casp8^{fl/fl}*, Mann-Whitney U test.

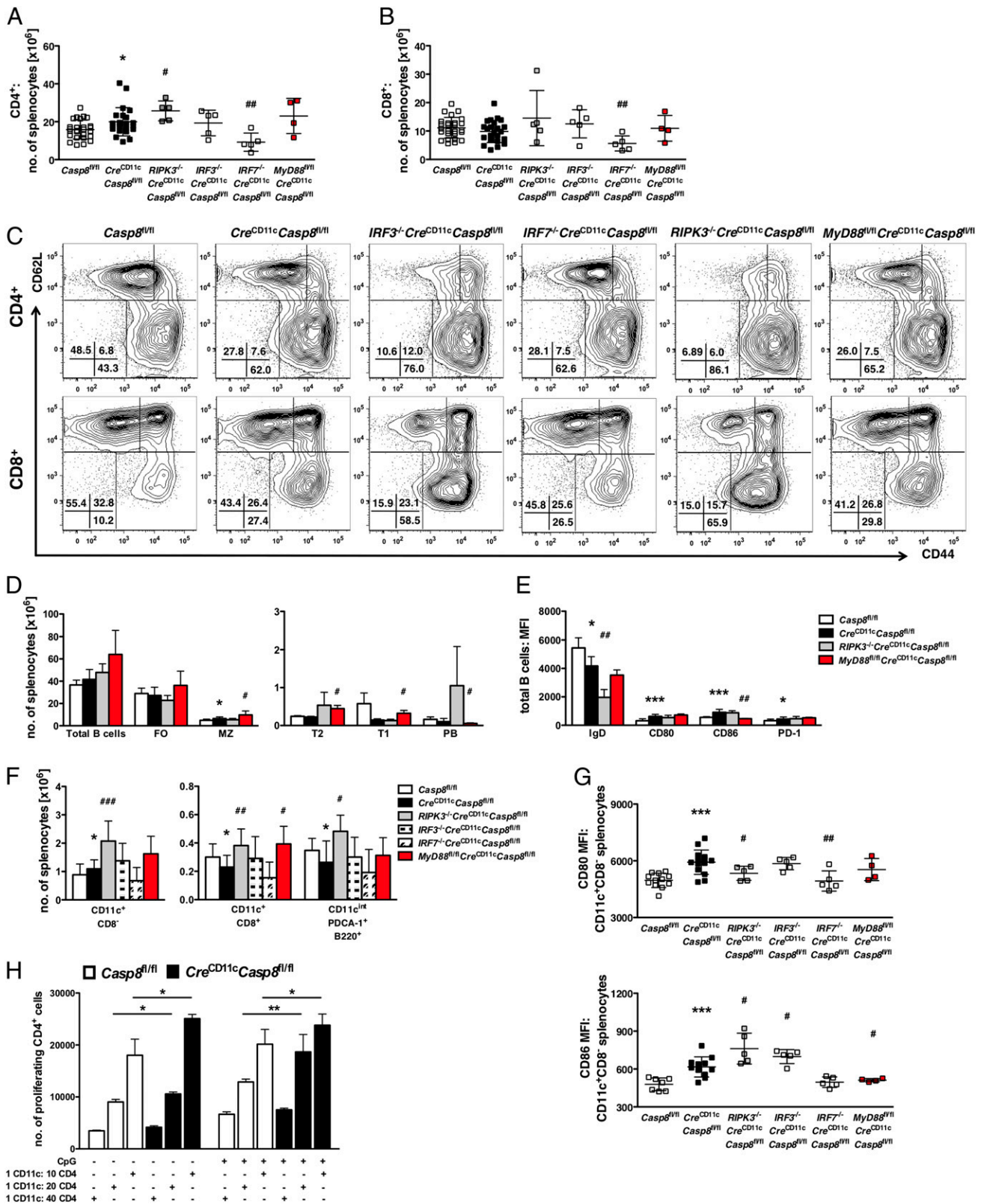


FIGURE 7. Caspase-8-deficient CD11c⁺CD8⁻ conventional DCs express increased activation markers and confer a hyperactive phenotype on lymphocytes. (A–G) Splenocytes from 6–8-mo-old female *Casp8^{fl/fl}* (control), *Cre^{CD11c}Casp8^{fl/fl}*, *RIPK3^{-/-}Cre^{CD11c}Casp8^{fl/fl}*, *IRF3^{-/-}Cre^{CD11c}Casp8^{fl/fl}*, *IRF7^{-/-}Cre^{CD11c}Casp8^{fl/fl}*, and *MyD88^{fl/fl}Cre^{CD11c}Casp8^{fl/fl}* mice ($n \geq 4$) were analyzed by flow cytometry. CD4⁺ (A) and CD8⁺ (B) T cell numbers. (C) Representative naive (CD44⁻CD62L⁺) and activated (CD44⁺CD62L⁻) T cell percentages of total CD4⁺ and CD8⁺ populations. (D) Total B cell (B220⁺) numbers and subsets: follicular (FO; CD19⁺CD21/35⁺CD23⁺), MZ (CD19⁺CD21/35⁺CD23^{low}), transitional 2 (T2; B220⁺AA4.1⁺CD23⁻), transitional 1 (T1; B220⁺AA4.1⁻CD23⁻), and plasmablasts (PB; CD19⁺B220^{low}CD138⁺CD21/35⁻CD23⁻). (E) B cell IgD, CD80, CD86, and PD-1 expression. (F) Conventional (CD11c⁺CD8⁻) and plasmacytoid (CD11c^{int}PDCA-1⁺B220⁺) DC numbers. (G) CD11c⁺CD8⁻ conventional DC CD80 and CD86 expression. (H) Bead-separated CD11c⁺ cells pulsed with OVA were cocultured with *OT-II/RAG^{-/-}* CD4⁺ T cells. Data are mean \pm SD. * $p < 0.05$, ** $p < 0.005$, *** $p < 0.0005$, control versus *Cre^{CD11c}Casp8^{fl/fl}*, Mann–Whitney U test. # $p < 0.05$, ## $p < 0.005$, ### $p < 0.0005$, *Cre^{CD11c}Casp8^{fl/fl}* versus experimental knockouts, Mann–Whitney U test.

expressed less PD-1 (Supplemental Fig. 4H) compared with *Cre^{CD11c}Casp8^{fl/fl}* T cells. MyD88 deletion also altered the B cell pool by augmenting the MZ, transitional 2, and transitional 1 subsets, reducing plasmablasts (Fig. 7D), and decreasing CD86 expression on total B cells compared with caspase-8 deficiency alone (Fig. 7E, Supplemental Fig. 4K). DC-specific loss of MyD88 led to increased numbers of CD11c⁺CD8⁺ conventional DCs compared with *Cre^{CD11c}Casp8^{fl/fl}* mice (Fig. 7F) and reduced CD11c⁺CD8⁻ conventional DC CD86 expression (Fig. 7G) to that of control DCs. Taken together, these results suggest that caspase-8 dampens MyD88 signaling in DCs; when caspase-8 is no longer present, unchecked signaling through this TLR mediator occurs, leading to the onset of systemic autoimmunity.

Discussion

Previous studies linked increased DC survival to the development of autoimmune disease. In this study, we show that *Cre^{CD11c}Casp8^{fl/fl}* mice develop splenomegaly, lymphadenopathy, autoantibodies, glomerulonephritis, immune complex deposition in the kidney, exacerbated proteinuria levels, heightened amounts of serum proinflammatory cytokines, and early mortality. In contrast to the other experimental models of apoptotic regulators in DCs, loss of caspase-8 in DCs does not affect their survival. There is no change in DC turnover rates, and there are equal numbers of *Cre^{CD11c}Casp8^{fl/fl}* and WT DCs in mixed bone marrow chimera mice. DCs lacking caspase-8 also fail to undergo apoptosis in response to FasL but are equally sensitive to etoposide-induced apoptosis. Thus, these data demonstrate that caspase-8 functions in a vastly different manner in DCs compared with Fas (14) or pan-caspase inhibitors (20).

Recently, a number of studies implicated caspase-8 in the regulation of the inflammasome, in particular the Nlrp3 inflammasome, independently of cell death in a number of cell types (29, 33, 34). Our findings are consistent with one such study (29), which showed that deletion of caspase-8 in DCs resulted in splenomegaly and lymphadenopathy through an apoptosis- and necroptosis-independent mechanism. Both studies show that caspase-8-deficient BMDCs secrete IL-1 β without the requirement for secondary ATP stimulation in response to TLR4 activation and that this is abrogated by the addition of necrostatin-1. However, our findings expand on the role of caspase-8 in DCs, because we show a novel necrostatin-1-specific inhibitory effect on proinflammatory cytokine secretion in response to TLR7/9 activation. In addition, we show that these changes are associated with the development of SLE-like disease, which results in early spontaneous mortality. Further, we show that the loss of caspase-8 in DCs leads to their hyperactivation that requires RIPK1 activity, and culminates in development of disease by a MyD88-dependent IRF3-independent mechanism. Differences between the studies may stem from differing cell-specific caspase-8 deletion constructs and/or the chosen transgenic CD11c-Cre line.

TLR7 and TLR9, which are intracellular receptors known to be activated by nucleic acids, have been linked to both human and murine models of SLE (35). TLR engagement induces RIPK signaling independent of DR activation, thereby leading to formation of a ripoptosome (10). Blocking RIPK1 kinase activity dampens TLR4/7/9-induced secretion of proinflammatory cytokines in caspase-8-deficient DCs without affecting cell survival. Thus, RIPK1 appears to function in a cell-specific manner that is vastly different based on the studies using T cell caspase-8-deficient mice (17). However, deletion of RIPK3 in *Cre^{CD11c}Casp8^{fl/fl}* mice is unable to reverse the observed phenotypic outcome, which is contrary to T cell caspase-8-deficient mice and similar to a recently published study (18, 29). Thus, our data substantiate a new

function for caspase-8, namely that it suppresses the inflammatory DC phenotype independent of activating apoptosis or inhibiting necroptosis but requires components of the ripoptosome.

Immunization studies revealed that T cell differentiation by DCs requires TLR activation (36). Teichmann et al. (37) found that deletion of DCs in a murine model of SLE ameliorates disease by limiting T cell expansion and subsequent kidney damage. Although most TLRs signal through MyD88, TLR3 requires the mediator TRIF, and TLR4 signals through both MyD88 and TRIF (38). Although DC-specific deletion of MyD88 in *MRL.Fas^{lpr}* mice reduces lymphoproliferation and controls dermatitis, nephritis development persisted (39). However, we were able to suppress lymphoproliferative and end-organ disease by cell-specific deletion of MyD88 in *Cre^{CD11c}Casp8^{fl/fl}* mice. Lyn is a Src family tyrosine kinase that phosphorylates caspase-8 and blocks its downstream activity in neutrophils (40). Although DC-specific deletion of Lyn mimics the systemic autoimmunity induced by deletion of caspase-8, these activities are independent of one another. However, similar to *Cre^{CD11c}Casp8^{fl/fl}* mice, DC-specific MyD88 deletion suppressed the autoimmunity induced in mice by DC-specific Lyn deficiency (41). These data indicate that both Lyn and caspase-8 limit MyD88-dependent TLR signaling in DCs. In contrast to *Cre^{CD11c}Casp8^{fl/fl}* mice, DC-specific deletion of MyD88 is unable to abrogate systemic inflammation caused by DC-specific FADD deficiency (42). Further, administration of broad-spectrum antibiotics suppresses systemic inflammation in DC-specific FADD-deficient mice (42) but has no effect in *Cre^{CD11c}Casp8^{fl/fl}* mice. These results suggest that, although caspase-8 and FADD together are intimately involved in cell death, caspase-8 mediates its suppressive action in DCs, in part, via a MyD88-dependent mechanism, whereas FADD may function to block MyD88-independent TLR signaling through TRIF. Our in vitro results suggest that the enzymatic activity of caspase-8 is dispensable for its suppressive activity, indicating that caspase-8 may act as a scaffolding protein that, in this case, may sequester MyD88. Future studies are required to define the exact interaction. Additionally, because we did not observe a complete abrogation of disease with MyD88 deletion, it is possible that caspase-8 also may dampen TRIF-dependent TLR signaling. Therefore, future studies are required to determine whether deletion of TRIF can ameliorate the systemic autoimmunity in *Cre^{CD11c}Casp8^{fl/fl}* mice.

A majority of SLE patients present an IFN signature, namely constitutive production of type I IFNs (IFN- α and IFN- β) and increased expression of type I IFN-regulated genes (12). This IFN signature is also detected in DCs from a murine model of SLE (43) and in mice lacking caspase-8 in DCs. Further, caspase-8-deficient BMDCs showed sustained DNA binding of IRF and IRF signaling response elements following extended TLR4/TLR7/TLR9 stimulation. These studies suggest that the loss of caspase-8 may increase the transcriptional activity of IRFs. Because previous studies showed that caspase-8 processes IRF3 for degradation (13), it would follow that IRF3 is elevated in the absence of caspase-8. Indeed, expression of IRF3 is increased in caspase-8-deficient BMDCs. Thus, we hypothesized that the presence of elevated levels of IRF3 in caspase-8-deficient DCs and the increased potential for deleterious transcriptional products may be the root cause of the autoimmunity observed in *Cre^{CD11c}Casp8^{fl/fl}* mice. However, to our surprise, deficiency in IRF3 exacerbates the lymphoproliferative disease in *Cre^{CD11c}Casp8^{fl/fl}* mice. These data indicate that IRF3 may be crucial in providing a compensatory mechanism to dampen inflammation induced by loss of caspase-8. Because recent evidence suggests that IRF3 acts not only as a transcription factor, but also as an apoptotic mediator through interaction with Bax via its newly discovered BH3 domain (44),

a failure to undergo apoptosis may be a potential explanation for the enhanced lymphoproliferative disease in *Cre^{CD11c}Casp8^{fl/fl}* mice. Although deletion of either IRF3 or IRF7 is unable to correct the inflammation associated with DC-specific caspase-8 deficiency, it is possible that other IRFs may be involved. For instance, IRF5 interacts with MyD88 downstream of TLR signaling and is phosphorylated and activated after TLR engagement (45). Further, polymorphisms in the IRF5 gene in SLE patients result in their constitutive expression, thereby upregulating type I IFN and proinflammatory cytokine production (46).

Both conventional and plasmacytoid DCs from patients with SLE were shown to possess abnormal phenotypes (47, 48). CD11c⁺ CD8⁻ conventional DCs from SLE patients display a more activated and mature phenotype, including enhanced MHC class II and costimulatory CD80/86 expression (49). Increased numbers of the other major DC subtype, plasmacytoid DCs, are seen in peripheral tissues of SLE patients (49). Furthermore, DCs from SLE patients fail to yield a tolerizing phenotype under experimental conditions (50) and produce high levels of proinflammatory IL-6, which is known to inhibit CD4⁺CD25⁺ regulatory T cells (51). These findings are recapitulated in DCs from mice with SLE-like disease; the number of DCs is increased, as is their secretion of proinflammatory cytokines (IL-12 and IL-6), cell surface activation and maturation markers, induction of T cell effector responses, and reduction of regulatory T cell function, compared with control DCs (52). Although these results support an important role for the expansion and activation of DCs in both human and murine models of SLE, the underlying mechanisms driving these changes are unknown. Our data suggest that in normal DCs, following TLR activation presumably via TLR4/7/9, caspase-8 associates with RIPK1 and MyD88 to limit their downstream signaling, thereby preventing the continuous activation of DCs. The removal of this break leads to a self-autoreactive loop in DCs and subsequent onset of autoimmune disease. Thus, our data document a critical role for caspase-8 in DCs in the pathogenesis of murine SLE-like disease and provide a link between caspase-8 and heightened TLR responses to endogenous ligands leading to disease pathogenesis. Future studies will be required to ascertain whether caspase-8 function or expression is reduced in DCs of SLE patients.

Acknowledgments

We thank the members of the Perlman Laboratory and Dr. Marcus Peter for helpful suggestions.

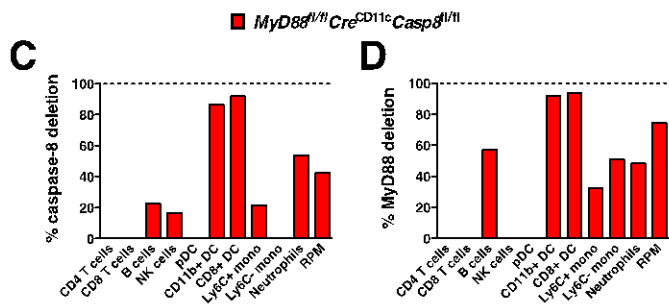
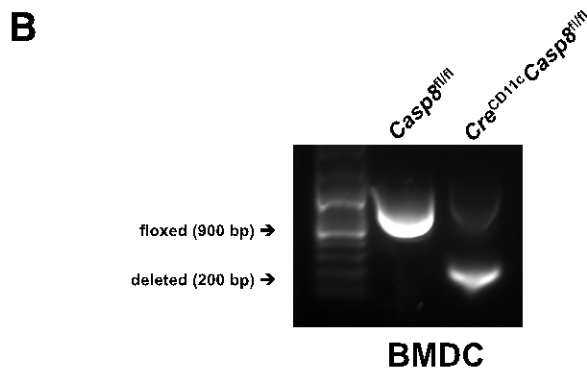
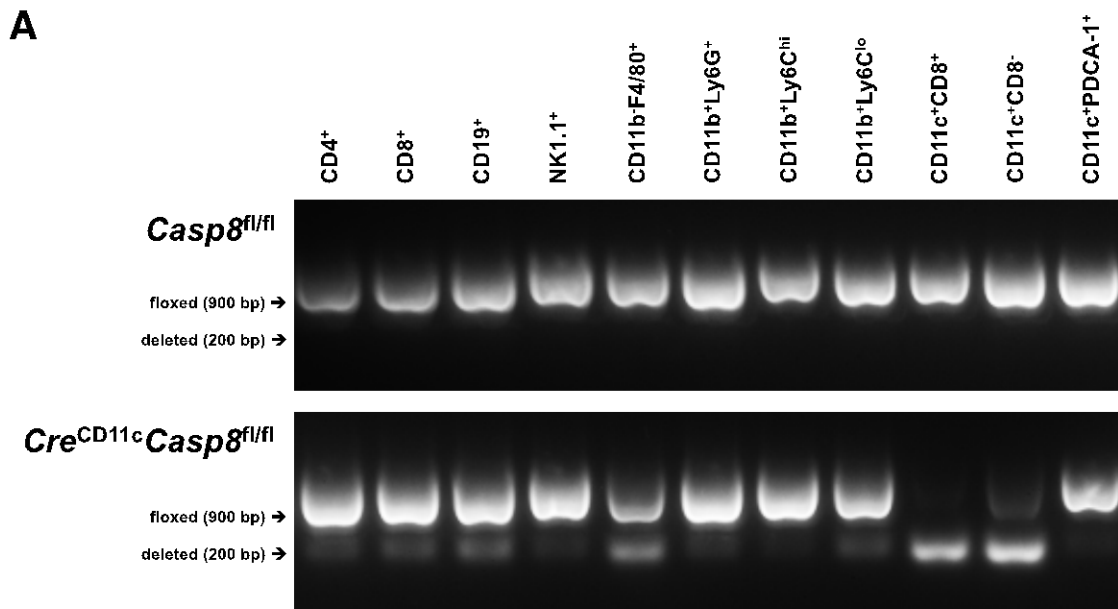
Disclosures

The authors have no financial conflicts of interest.

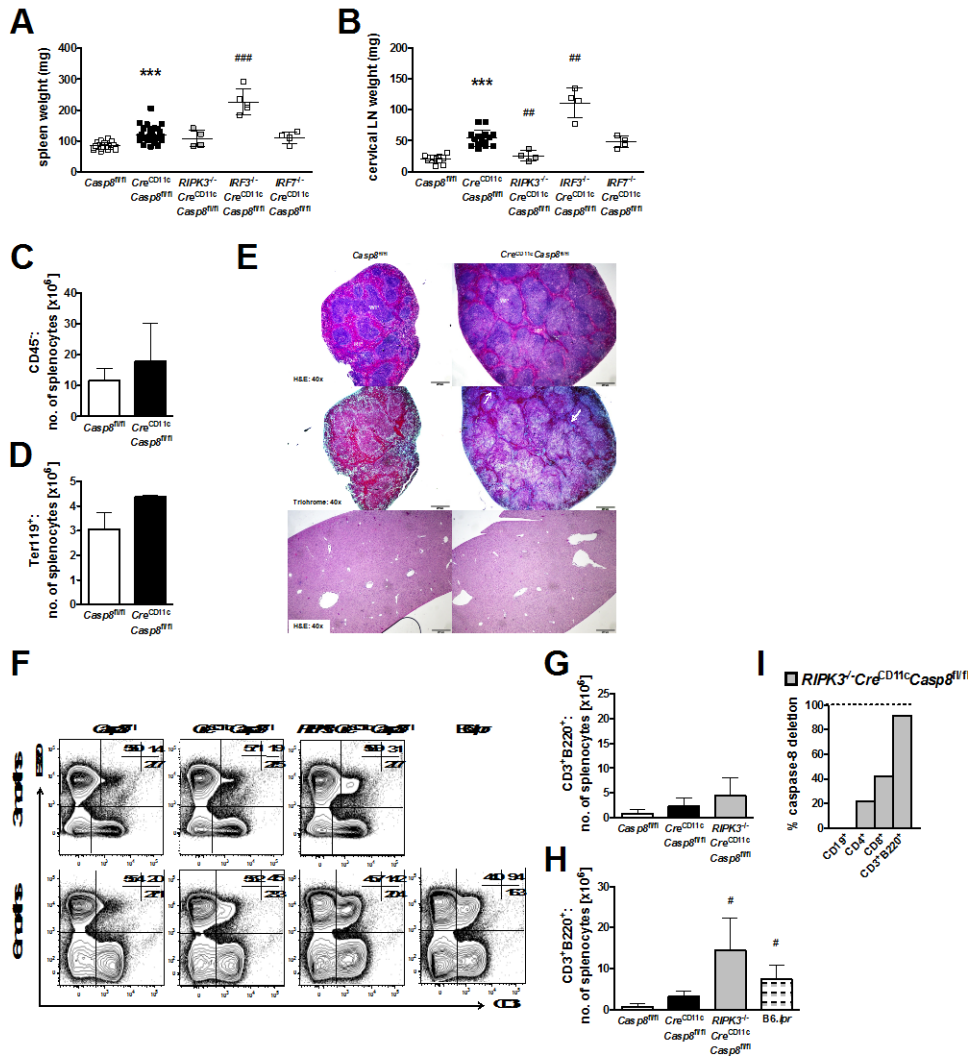
References

- Hutcheson, J., and H. Perlman. 2008. BH3-only proteins in rheumatoid arthritis: potential targets for therapeutic intervention. *Oncogene* 27(Suppl. 1): S168–S175.
- Oberst, A., C. P. Dillon, R. Weinlich, L. L. McCormick, P. Fitzgerald, C. Pop, R. Hakem, G. S. Salvesen, and D. R. Green. 2011. Catalytic activity of the caspase-8-FLIP(L) complex inhibits RIPK3-dependent necrosis. *Nature* 471: 363–367.
- Helfer, B., B. C. Boswell, D. Finlay, A. Cipres, K. Vuori, T. Bong Kang, D. Wallach, A. Dorfleutner, J. M. Lahti, D. C. Flynn, and S. M. Frisch. 2006. Caspase-8 promotes cell motility and calpain activity under nonapoptotic conditions. *Cancer Res.* 66: 4273–4278.
- Dohrman, A., T. Kataoka, S. Cuenin, J. Q. Russell, J. Tschopp, and R. C. Budd. 2005. Cellular FLIP (long form) regulates CD8⁺ T cell activation through caspase-8-dependent NF-kappa B activation. *J. Immunol.* 174: 5270–5278.
- Rajput, A., A. Kovalenko, K. Bogdanov, S. H. Yang, T. B. Kang, J. C. Kim, J. Du, and D. Wallach. 2011. RIG-I RNA helicase activation of IRF3 transcription factor is negatively regulated by caspase-8-mediated cleavage of the RIP1 protein. *Immunity* 34: 340–351.
- Kovalenko, A., J. C. Kim, T. B. Kang, A. Rajput, K. Bogdanov, O. Dittrich-Breiholz, M. Kracht, O. Brenner, and D. Wallach. 2009. Caspase-8 deficiency in epidermal keratinocytes triggers an inflammatory skin disease. *J. Exp. Med.* 206: 2161–2177.
- Hu, W. H., H. Johnson, and H. B. Shu. 2000. Activation of NF-kappaB by FADD, Casper, and caspase-8. *J. Biol. Chem.* 275: 10838–10844.
- Oberst, A., and D. R. Green. 2011. It cuts both ways: reconciling the dual roles of caspase 8 in cell death and survival. *Nat. Rev. Mol. Cell Biol.* 12: 757–763.
- Mocarski, E. S., J. W. Upton, and W. J. Kaiser. 2012. Viral infection and the evolution of caspase 8-regulated apoptotic and necrotic death pathways. *Nat. Rev. Immunol.* 12: 79–88.
- Feoktistova, M., P. Geserick, B. Kellert, D. P. Dimitrova, C. Langlais, M. Hupe, K. Cain, M. MacFarlane, G. Häcker, and M. Leverkus. 2011. cIAPs block Ripoptosome formation, a RIP1/caspase-8 containing intracellular cell death complex differentially regulated by cFLIP isoforms. *Mol. Cell* 43: 449–463.
- Vince, J. E., W. W. Wong, I. Gentle, K. E. Lawlor, R. Allam, L. O'Reilly, K. Mason, O. Gross, S. Ma, G. Guarda, et al. 2012. Inhibitor of apoptosis proteins limit RIP3 kinase-dependent interleukin-1 activation. *Immunity* 36: 215–227.
- Rönnblom, L., and V. Pascual. 2008. The innate immune system in SLE: type I interferons and dendritic cells. *Lupus* 17: 394–399.
- Sears, N., G. C. Sen, G. R. Stark, and S. Chattopadhyay. 2011. Caspase-8-mediated cleavage inhibits IRF-3 protein by facilitating its proteasome-mediated degradation. *J. Biol. Chem.* 286: 33037–33044.
- Stranges, P. B., J. Watson, C. J. Cooper, C. M. Choisy-Rossi, A. C. Stonebraker, R. A. Beighton, H. Hartig, J. P. Sundberg, S. Servick, G. Kaufmann, et al. 2007. Elimination of antigen-presenting cells and autoreactive T cells by Fas contributes to prevention of autoimmunity. *Immunity* 26: 629–641.
- Hao, Z., G. S. Duncan, J. Seagal, Y. W. Su, C. Hong, J. Haight, N. J. Chen, A. Elia, A. Wakeham, W. Y. Li, et al. 2008. Fas receptor expression in germinal-center B cells is essential for T and B lymphocyte homeostasis. *Immunity* 29: 615–627.
- Hao, Z., B. Hampel, H. Yagita, and K. Rajewsky. 2004. T cell-specific ablation of Fas leads to Fas ligand-mediated lymphocyte depletion and inflammatory pulmonary fibrosis. *J. Exp. Med.* 199: 1355–1365.
- Strasser, A., P. J. Jost, and S. Nagata. 2009. The many roles of FAS receptor signaling in the immune system. *Immunity* 30: 180–192.
- Ch'en, I. L., J. S. Tsau, J. D. Molkenin, M. Komatsu, and S. M. Hedrick. 2011. Mechanisms of necroptosis in T cells. *J. Exp. Med.* 208: 633–641.
- Kaiser, W. J., J. W. Upton, A. B. Long, D. Livingston-Rosanoff, L. P. Daley-Bauer, R. Hakem, T. Caspary, and E. S. Mocarski. 2011. RIP3 mediates the embryonic lethality of caspase-8-deficient mice. *Nature* 471: 368–372.
- Chen, M., Y. H. Wang, Y. Wang, L. Huang, H. Sandoval, Y. J. Liu, and J. Wang. 2006. Dendritic cell apoptosis in the maintenance of immune tolerance. *Science* 311: 1160–1164.
- Beisner, D. R., I. L. Ch'en, R. V. Kolla, A. Hoffmann, and S. M. Hedrick. 2005. Cutting edge: innate immunity conferred by B cells is regulated by caspase-8. *J. Immunol.* 175: 3469–3473.
- Hutcheson, J., J. C. Scatizzi, A. M. Siddiqui, G. K. Haines, III, T. Wu, Q. Z. Li, L. S. Davis, C. Mohan, and H. Perlman. 2008. Combined deficiency of proapoptotic regulators Bim and Fas results in the early onset of systemic autoimmunity. *Immunity* 28: 206–217.
- Cuda, C. M., H. Agrawal, A. V. Misharin, G. K. Haines, III, J. Hutcheson, E. Weber, J. A. Schoenfeldt, C. Mohan, R. M. Pope, and H. Perlman. 2012. Requirement of myeloid cell-specific Fas expression for prevention of systemic autoimmunity in mice. *Arthritis Rheum.* 64: 808–820.
- Rose, S., A. Misharin, and H. Perlman. 2012. A novel Ly6C/Ly6G-based strategy to analyze the mouse splenic myeloid compartment. *Cytometry A* 81: 343–350.
- Labeur, M. S., B. Roters, B. Pers, A. Mehling, T. A. Luger, T. Schwarz, and S. Grabbe. 1999. Generation of tumor immunity by bone marrow-derived dendritic cells correlates with dendritic cell maturation stage. *J. Immunol.* 162: 168–175.
- Scatizzi, J. C., M. Mavers, J. Hutcheson, B. Young, B. Shi, R. M. Pope, E. M. Ruderman, D. S. Samways, J. A. Corbett, T. M. Egan, and H. Perlman. 2009. The CDK domain of p21 is a suppressor of IL-1beta-mediated inflammation in activated macrophages. *Eur. J. Immunol.* 39: 820–825.
- Ashany, D., A. Savir, N. Bhardwaj, and K. B. Elkon. 1999. Dendritic cells are resistant to apoptosis through the Fas (CD95/APO-1) pathway. *J. Immunol.* 163: 5303–5311.
- Guo, Z., M. Zhang, H. An, W. Chen, S. Liu, J. Guo, Y. Yu, and X. Cao. 2003. Fas ligation induces IL-1beta-dependent maturation and IL-1beta-independent survival of dendritic cells: different roles of ERK and NF-kappaB signaling pathways. *Blood* 102: 4441–4447.
- Kang, T. B., S. H. Yang, B. Toth, A. Kovalenko, and D. Wallach. 2013. Caspase-8 blocks kinase RIPK3-mediated activation of the NLRP3 inflammasome. *Immunity* 38: 27–40.
- Cohen, P. L., and R. A. Eisenberg. 1991. Lpr and gld: single gene models of systemic autoimmunity and lymphoproliferative disease. *Annu. Rev. Immunol.* 9: 243–269.
- Takahashi, N., L. Duprez, S. Grootjans, A. Cauwels, W. Nerinckx, J. B. DuHadaway, V. Goossens, R. Roelandt, F. Van Hauwermeiren, C. Libert, et al. 2012. Necrostatin-1 analogues: critical issues on the specificity, activity and in vivo use in experimental disease models. *Cell Death Dis.* 3: e437.
- Mathis, D., and C. Benoist. 2011. Microbiota and autoimmune disease: the hosted self. *Cell Host Microbe* 10: 297–301.
- Gurung, P., P. K. Anand, R. K. Malireddi, L. Vande Walle, N. Van Opdenbosch, C. P. Dillon, R. Weinlich, D. R. Green, M. Lamkanfi, and T. D. Kanneganti. 2014. FADD and caspase-8 mediate priming and activation of the canonical and noncanonical Nlrp3 inflammasomes. *J. Immunol.* 192: 1835–1846.

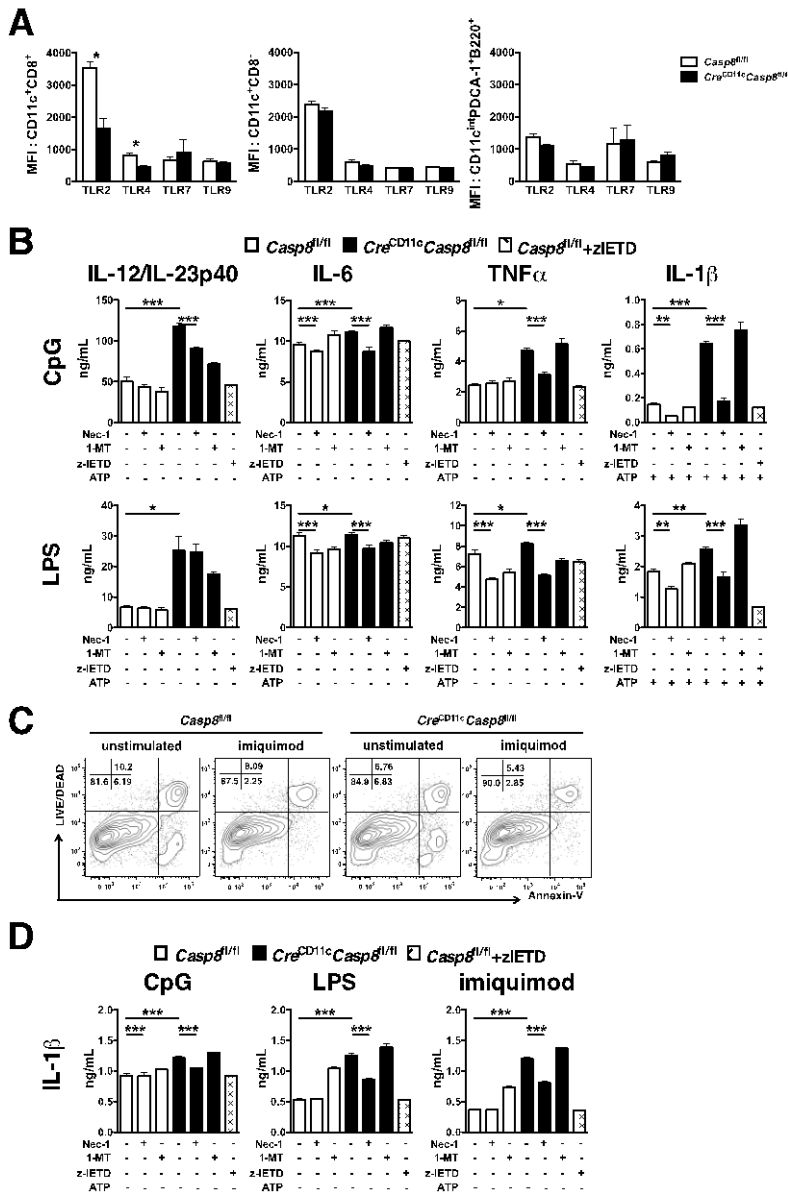
34. Shenderov, K., N. Riteau, R. Yip, K. D. Mayer-Barber, S. Oland, S. Hieny, P. Fitzgerald, A. Oberst, C. P. Dillon, D. R. Green, et al. 2014. Cutting edge: Endoplasmic reticulum stress licenses macrophages to produce mature IL-1 β in response to TLR4 stimulation through a caspase-8- and TRIF-dependent pathway. *J. Immunol.* 192: 2029–2033.
35. Celhar, T., R. Magalhães, and A. M. Fairhurst. 2012. TLR7 and TLR9 in SLE: when sensing self goes wrong. *Immunol. Res.* 53: 58–77.
36. Joffre, O., M. A. Nolte, R. Spörri, and C. Reis e Sousa. 2009. Inflammatory signals in dendritic cell activation and the induction of adaptive immunity. *Immunol. Rev.* 227: 234–247.
37. Teichmann, L. L., M. L. Ols, M. Kashgarian, B. Reizis, D. H. Kaplan, and M. J. Shlomchik. 2010. Dendritic cells in lupus are not required for activation of T and B cells but promote their expansion, resulting in tissue damage. *Immunity* 33: 967–978.
38. West, A. P., A. A. Koblansky, and S. Ghosh. 2006. Recognition and signaling by toll-like receptors. *Annu. Rev. Cell Dev. Biol.* 22: 409–437.
39. Teichmann, L. L., D. Schenten, R. Medzhitov, M. Kashgarian, and M. J. Shlomchik. 2013. Signals via the adaptor MyD88 in B cells and DCs make distinct and synergistic contributions to immune activation and tissue damage in lupus. *Immunity* 38: 528–540.
40. Jia, S. H., J. Parodo, A. Kapus, O. D. Rotstein, and J. C. Marshall. 2008. Dynamic regulation of neutrophil survival through tyrosine phosphorylation or dephosphorylation of caspase-8. *J. Biol. Chem.* 283: 5402–5413.
41. Lamagna, C., P. Scapini, J. A. van Ziffle, A. L. DeFranco, and C. A. Lowell. 2013. Hyperactivated MyD88 signaling in dendritic cells, through specific deletion of Lyn kinase, causes severe autoimmunity and inflammation. *Proc. Natl. Acad. Sci. USA* 110: E3311–E3320.
42. Young, J. A., T. H. He, B. Reizis, and A. Winoto. 2013. Commensal microbiota are required for systemic inflammation triggered by necrotic dendritic cells. *Cell Rep.* 3: 1932–1944.
43. Sriram, U., L. Varghese, H. L. Bennett, N. R. Jog, D. K. Shivers, Y. Ning, E. M. Behrens, R. Caricchio, and S. Gallucci. 2012. Myeloid dendritic cells from B6.NZM Sle1/Sle2/Sle3 lupus-prone mice express an IFN signature that precedes disease onset. *J. Immunol.* 189: 80–91.
44. Chattopadhyay, S., and G. C. Sen. 2010. IRF-3 and Bax: a deadly affair. *Cell Cycle* 9: 2479–2480.
45. Paun, A., and P. M. Pitha. 2007. The IRF family, revisited. *Biochimie* 89: 744–753.
46. Feng, D., R. C. Stone, M. L. Eloranta, N. Sangster-Guity, G. Nordmark, S. Sigurdsson, C. Wang, G. Alm, A. C. Syvänen, L. Rönnblom, and B. J. Barnes. 2010. Genetic variants and disease-associated factors contribute to enhanced interferon regulatory factor 5 expression in blood cells of patients with systemic lupus erythematosus. *Arthritis Rheum.* 62: 562–573.
47. Kis-Toth, K., and G. C. Tsokos. 2010. Dendritic cell function in lupus: Independent contributors or victims of aberrant immune regulation. *Autoimmunity* 43: 121–130.
48. Monrad, S., and M. J. Kaplan. 2007. Dendritic cells and the immunopathogenesis of systemic lupus erythematosus. *Immunol. Res.* 37: 135–145.
49. Chan, V. S., Y. J. Nie, N. Shen, S. Yan, M. Y. Mok, and C. S. Lau. 2012. Distinct roles of myeloid and plasmacytoid dendritic cells in systemic lupus erythematosus. *Autoimmun. Rev.* 11: 890–897.
50. Berkun, Y., I. Verbovetski, A. Ben-Ami, D. Paran, D. Caspi, A. Krispin, U. Trahtemberg, O. Gill, Y. Naparstek, and D. Mevorach. 2008. Altered dendritic cells with tolerizing phenotype in patients with systemic lupus erythematosus. *Eur. J. Immunol.* 38: 2896–2904.
51. Decker, P., I. Kötter, R. Klein, B. Berner, and H. G. Rammensee. 2006. Monocyte-derived dendritic cells over-express CD86 in patients with systemic lupus erythematosus. *Rheumatology (Oxford)* 45: 1087–1095.
52. Sang, A., Y. Yin, Y. Y. Zheng, and L. Morel. 2012. Animal models of molecular pathology systemic lupus erythematosus. *Prog. Mol. Biol. Transl. Sci.* 105: 321–370.



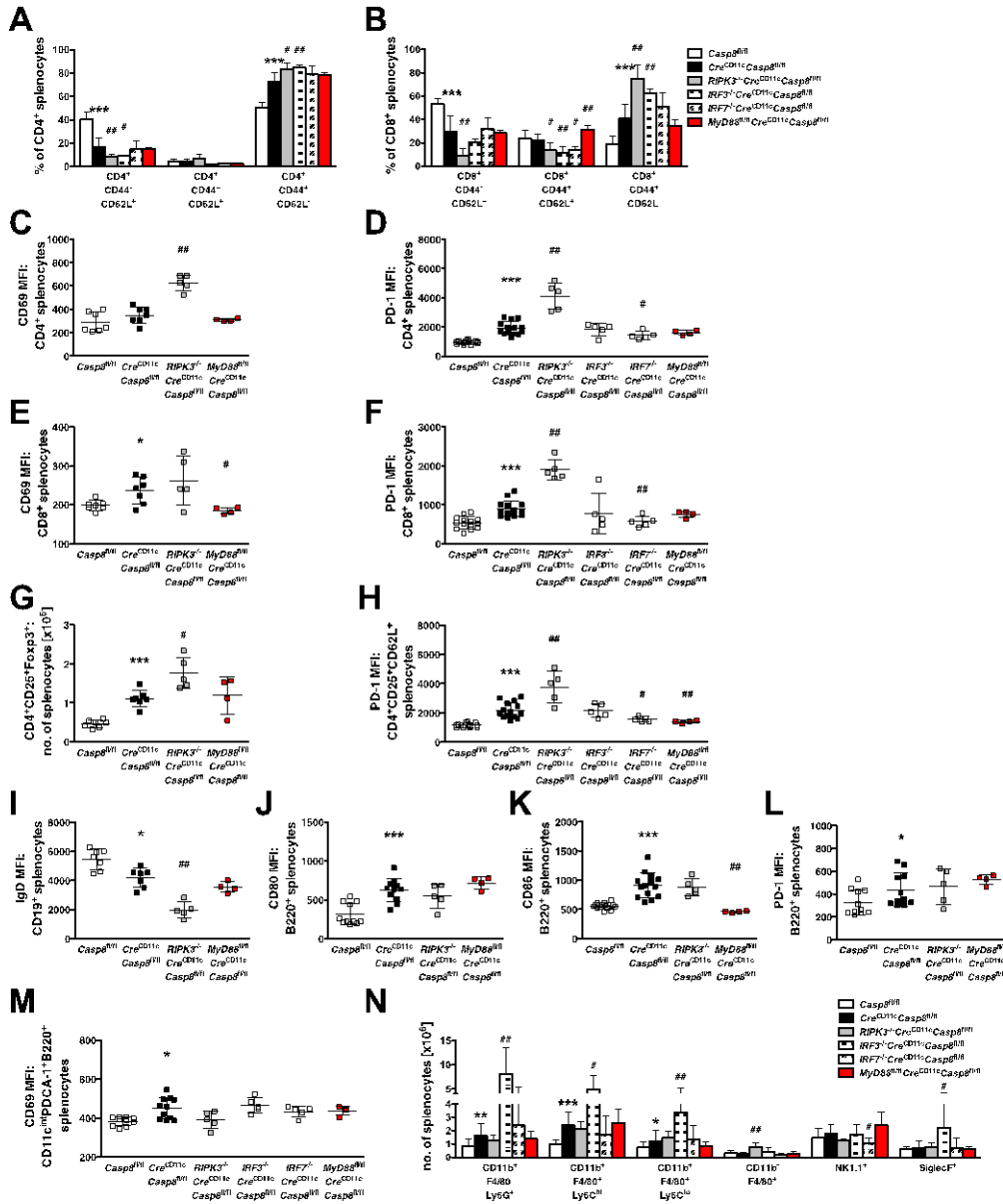
Supplemental Figure 1. PCR for genotype validation. (A) Splenocyte populations from *Cre*^{CD11c}*Casp8*^{fl/fl} mice were sorted as: B cells (CD19⁺), CD4⁺ and CD8⁺ T cells, NK cells (NK1.1⁺), red pulp macrophages (CD11b⁺F4/80⁺), neutrophils (CD11b⁺Ly6G⁺), monocytes/macrophages (CD11b⁺CD11c^{low/negative}SSC^{low}F4/80^{low}) further subdivided into Ly6C⁻ and Ly6C⁺, pDC (mPDCA-1⁺B220⁺CD11c^{intermediate}) and conventional DC (B220⁻CD11c⁺CD8⁺ and B220⁻CD11c⁺CD8⁻), and subjected to PCR for *Casp8*^{fl/fl} and *Casp8*^{del} alleles. (B) BMDCs generated from *Cre*^{CD11c}*Casp8*^{fl/fl} mice were subjected to PCR for *Casp8*^{fl/fl} and *Casp8*^{del} alleles. (C-D) Splenocyte populations from *MyD88*^{fl/fl}*Cre*^{CD11c}*Casp8*^{fl/fl} mice were sorted as in (A) and subjected to real time PCR for (C) *caspase-8* and (D) *MyD88* deletion.



Supplemental Figure 2. Phenotypes of young and aged mice. (A-B) 2-3-month-old female *Casp8*^{fl/fl} (control), *Cre*^{CD11c}*Casp8*^{fl/fl}, *RIPK3*^{-/-}*Cre*^{CD11c}*Casp8*^{fl/fl}, *IRF3*^{-/-}*Cre*^{CD11c}*Casp8*^{fl/fl} and *IRF7*^{-/-}*Cre*^{CD11c}*Casp8*^{fl/fl} mice (n≥4) were evaluated for (A) spleen and (B) cervical lymph node weights. (C-E) 6-8-month-old control and *Cre*^{CD11c}*Casp8*^{fl/fl} mice (n≥7) were evaluated for numbers of (C) CD45⁺ and (D) Ter119⁺ splenocytes. (E) Representative formalin-fixed spleen sections (4 μm) stained with hematoxylin and eosin (H&E) and trichrome and formalin-fixed liver sections (4 μm) stained with H&E. (F-H) Splenocytes from 3- and 6-month-old control, *Cre*^{CD11c}*Casp8*^{fl/fl}, *RIPK3*^{-/-}*Cre*^{CD11c}*Casp8*^{fl/fl} and B6.*lpr* mice (n≥5) were analyzed by flow cytometry. (F) Representative CD4⁺CD8⁺CD3⁺B220⁺ T-cell percentages of total splenocytes at 3 and 6 months. Numbers of CD4⁺CD8⁺CD3⁺B220⁺ double negative T-cells at (G) 3 and (H) 6 months. (I) Splenocyte populations were sorted as: B-cells (CD19⁺), CD4⁺, CD8⁺ and DN T-cells (CD4⁺CD8⁺CD3⁺B220⁺) and subjected to real time PCR for *caspase-8* deletion. Data are represented as mean ± SD and compared by Mann Whitney test. * denotes comparison between control and *Cre*^{CD11c}*Casp8*^{fl/fl}, # denotes comparison between *Cre*^{CD11c}*Casp8*^{fl/fl} and *RIPK3*^{-/-}*Cre*^{CD11c}*Casp8*^{fl/fl}, B6.*lpr*, *IRF3*^{-/-}*Cre*^{CD11c}*Casp8*^{fl/fl} or *IRF7*^{-/-}*Cre*^{CD11c}*Casp8*^{fl/fl}. *, #:p<0.05; **, ###:p<0.005; ***, ####:p<0.0005.



Supplemental Figure 3. TLR ligation does not induce cell death. (A) Splenocytes from 6-8 month-old *Casp8^{fl/fl}* (control) and *Cre^{CD11c}Casp8^{fl/fl}* ($n \geq 5$) were analyzed by flow cytometry for expression of TLRs. (B) GM-CSF + Flt3-L-treated BMDCs from control and *Cre^{CD11c}Casp8^{fl/fl}* mice were stimulated with CpG or LPS \pm Nec-1 and/or zIETD-FMK (zIETD), a caspase-8 inhibitor and/or 1-Methyl-D-tryptophan (1-MT) for 6 hours \pm ATP (5mM) and supernatants evaluated for IL-12/IL-23p40, IL-6, TNF α , and IL-1 β . (C) Control and *Cre^{CD11c}Casp8^{fl/fl}* BMDCs were stimulated with imiquimod (5 μ g/mL) for 6 hours and cells were stained with Annexin-V and Aqua live/dead. Representative percentages of Annexin-V- and LIVE/DEAD-stained BMDCs. (D) GM-CSF + Flt3-L-treated BMDCs from control and *Cre^{CD11c}Casp8^{fl/fl}* mice were stimulated with CpG, LPS or imiquimod \pm Nec-1 and/or zIETD-FMK (zIETD) and/or 1-Methyl-D-tryptophan (1-MT) for 6 hours \pm ATP (5mM) and supernatants evaluated for IL-1 β . Data are represented as mean \pm SD and compared by Mann Whitney test.



Supplemental Figure 4. Alterations in splenic populations. (A-L) Splenocytes from 6-8-month-old *Casp8^{fl/fl}* (control), *Cre^{CD11c}Casp8^{fl/fl}*, *RIPK3^{-/-}Cre^{CD11c}Casp8^{fl/fl}*, *IRF3^{-/-}Cre^{CD11c}Casp8^{fl/fl}* and *IRF7^{-/-}Cre^{CD11c}Casp8^{fl/fl}* mice ($n \geq 4$) were analyzed by flow cytometry. Naive ($CD44^-CD62L^+$), memory ($CD44^+CD62L^+$) and effector ($CD44^+CD62L^-$) (A) $CD4^+$ T-cell and (B) $CD8^+$ T-cell numbers. $CD4^+$ (C) CD69 and (D) PD-1 expression levels and $CD8^+$ T-cell (E) CD69 and (F) PD-1 expression levels. Regulatory T-cell ($CD4^+CD25^+Foxp3^+$) (G) numbers and (H) PD-1 expression level. Total B-cell (I) IgD, (J) CD80, (K) CD86 and (L) PD-1 expression levels. (M) plasmacytoid DC ($CD11c^{int}PDCA-1^+B220^+$) CD69 expression. (N) Neutrophil ($CD11b^+F4/80^+Ly6G^+$), $Ly6C^{high}$ macrophage ($CD11b^+F4/80^+$), $Ly6C^{low}$ macrophage ($CD11b^+F4/80^+$), red pulp macrophage ($CD11b^+F4/80^+$), NK ($NK1.1^+$) and eosinophil ($SiglecF^+$) cell numbers. Data are represented as mean \pm SD and compared by Mann Whitney test. * denotes comparison between control and *Cre^{CD11c}Casp8^{fl/fl}*, # denotes comparison between *Cre^{CD11c}Casp8^{fl/fl}* and experimental knockouts. *, #: $p < 0.05$; **, ###: $p < 0.005$; ***, ####: $p < 0.0005$.